This document is the accepted manuscript version of the following article: Feurer, T., Reinhard, P., Avancini, E., Bissig, B., Löckinger, J., Fuchs, P., … Tiwari, A. N. (2017). Progress in thin film CIGS photovoltaics – research and development, manufacturing, and applications. Progress in Photovoltaics, 25(7), 645-667. http://doi.org/10.1002/pip.2811

Progress in Thin Film CIGS Photovoltaics – R&D, Manufacturing and Applications

Authors: Thomas Feurer[1], Patrick Reinhard[2], Enrico Avancini[1], Benjamin Bissig[1], Johannes Löckinger[1], Peter Fuchs[1], Romain Carron[1], Thomas Paul Weiss[1], Julian Perrenoud[2], Stephan Stutterheim[2], Stephan Buecheler[1], Ayodhya N. Tiwari[1]

[1] Laboratory for Thin Films and Photovoltaics, Empa - Swiss Federal Laboratories for Materials Science and Technology, Ueberlandstrasse 129, 8600 Duebendorf, Switzerland

[2] Flisom AG, Überlandstrasse 129, 8600 Dübendorf, Switzerland

Abstract

This review summarizes the current status of $Cu(In,Ga)(S,Se)_2$ (CIGS) thin film solar cell technology with a focus on recent advancements and emerging concepts intended for higher efficiency and novel applications. The recent developments and trends of research in labs and industrial achievements communicated within the last years are reviewed and the major developments linked to alkali post deposition treatment and composition grading in CIGS, surface passivation, buffer and transparent contact layers are emphasized. Encouraging results have been achieved for CIGS based tandem solar cells and for improvement in low light device performance. Challenges of technology transfer of lab's record high efficiency cells to average industrial production are obvious from the reported efficiency values. One section is dedicated to development and opportunities offered by flexible and lightweight CIGS modules.

Introduction

$Cu(In,Ga)(S,Se)_2$ (CIGS)-based thin film solar cells represent one of the most promising photovoltaic technology, with steadily increasing champion cell efficiencies up to 22.6%[1] reported for laboratory scale absorbers. Efficiencies above 20% have been achieved on rigid and flexible substrates by different research institutes as well as industrial companies (see overview in Table 1+2). Key advantages of CIGS compared to other conventional photovoltaic technologies include the high energy yield (kWh/KWp installed), low temperature coefficient of power loss, low sensitivity to shadowing and short energy payback time [2–4]. Cost-projections down to 0.35 Euro/Wp have been announced for the current technology, with potential for further reduction upon scale-up, allowing a significant reduction of the total system cost [5].

The possibility to grow thin films of large area absorber onto a glass as well as lightweight, flexible substrates opens up the field for low-cost manufacturing methods as

well as new applications. Applications such as building-integrated PV (BIPV), transport-integrated PV (TIPV), space flight or any mobile power generation are market segments where those type of solar modules have greatest advantage compared with traditional PV technologies [6].

In the following, we use CIGS as a general abbreviation for chalcopyrite based solar cells when no specific compositional information is required. The more stringent notation (CIGSe for $Cu(In,Ga)Se_2$ or CIGSSe for $Cu(In, Ga)(S, Se)_2$) is used if differentiation is needed.

Device structure

Figure 1 shows the typical structure of a CIGS solar cell, indicating some commonly used materials for the different layers. A more detailed description is available elsewhere [7–9]. The most commonly used substrate is rigid, 3-4mm thick soda-lime glass (SLG), as it is thermally stable, chemically inert, has a similar thermal expansion coefficient as the absorber. It also has a smooth surface, insulating properties suitable for monolithic interconnection and can supply alkali elements for high efficient cells (see section “Alkali post deposition treatment of CIGS layer”). However a significant amount of work has also been done for CIGS on flexible substrates such as metal foils, ceramics and polymer films, as discussed in more detail elsewhere [7].

The preferred back contact consists of sputtered molybdenum, serving as a quasi-ohmic contact with the absorber by formation of a $MoSe_2$ intermediate layer during absorber growth. The p-type CIGS absorber can be grown by co-evaporation processes, with selenization followed by sulfurization of precursors deposited by sputtering, electrodeposition or printing. While co-evaporation led to the highest efficiencies for a long time [10–12], the largest commercial manufacturer and current world record holder Solar Frontier is using a sputtered precursor with subsequent selenization and sulfurization and reported a record efficiency of 22.3% [13,14]. Table 1 and 2 gives a selected overview of the growth method and efficiencies achieved in different research institutes and companies. Various CIGS compositions are used, mainly aiming at tuning the material band gap (In-Ga ratio, Se-S ratio), as well as its bulk and surface electronic properties. Among others, the introduction of a band gap grading and the presence of alkali elements are two key features that have fueled the development of higher efficiencies in recent years and are addressed in more detail in the following sections.

Following the absorber deposition, heterojunction formation is ensured by the deposition of a thin n-type buffer layer. Historically, CdS has been used for best efficiency, but due to its relatively low band gap (2.4 eV) the search for alternative materials yielding similar junction quality has been given much attention and is discussed further below (see section “Buffer layers”).

Transparent conducting oxides (TCO) are applied as the front contact. Research cells and even some commercial module designs support the charge collection with an additional metallic grid. A typical TCO stack consists of a thin layer of intrinsic zinc oxide followed by aluminum-doped zinc oxide [15]. The intrinsic layer helps preventing current leakage in case of local inhomogeneities or incomplete buffer coverage [16,17] and also possibly to protect the buffer from ion damage during TCO sputtering.

For record efficiency cells and modules an anti-reflecting coating is often applied.

Some recent advancements

Alkali post deposition treatment of CIGS layer

Addition of alkali elements, especially Na, has long been subject of studies in the chalcopyrite thin film community, due to the beneficial impact on the electronic properties of the absorber and solar cells. If not diffusing directly from the glass substrate during the absorber deposition at elevated temperature [18], similar beneficial effect on the bulk electronic properties were observed when adding them in a controlled manner prior, during or after CIGS growth [19]. Whereas Na long showed the most beneficial effect, the controlled addition of KF in a post-deposition treatment (PDT) yielded a significant improvement in efficiency up to a world record efficiency of 20.4% [10]. Such a PDT treatment was originally found to be the most beneficial method to add Na onto CIGS grown at low-temperature on plastic substrate [20], because it allows separating the influence of Na on CIGS film growth from its beneficial effect on electronic properties. While it was found that Na PDT mainly modifies the bulk electronic properties of the CIGS layer, with no discernible surface modification, addition of KF in a similar PDT treatment leads to a significant alteration of the CIGS surface composition, namely Cu and Ga depletion. Furthermore, a decrease in Na content for samples treated with K is also systematically observed [10,21–23], possibly based on an ion exchange mechanism. The modified CIGS surface has strong implications on the interface formation and growth of subsequent layers, especially when grown by chemical bath methods [10,24]. A review of the impact of addition of KF after the growth of CIGS is presented in ref. [25]. Strengthened by several consecutive world records for the CIGS technology when applying a process based on alkali-addition after CIGS growth [12,26,27], this findings shed new light on the importance of considering the alkali addition *process* together with alkali type and their combination and the effects on both bulk as well as surface/interface properties of CIGS and solar cells. Whether the effect of KF PDT is a direct electronic effect due to the modified surface composition of the CIGS layer or whether it indirectly affects the

junction quality by modifying the interface properties during buffer layer deposition is still under discussion. Influence on the bulk properties have also to be considered and cannot be excluded from the overall effects on solar cell efficiency.

In addition to the 1-dimensional vision of the buffer layer-absorber formation, the formation of point contacts induced by a nano-structuring of the interface could shift the transport characteristics of the carriers from a 1-dimensional to a 2-dimensional model [28]. Overall, the fact that the KF PDT is not only beneficial for co-evaporated absorbers, but also for sputtered and selenized films [22], and even for absorbers with higher Ga content [26], hints that it likely is mostly an interface-related improvement. Latest results using the heavier alkali elements rubidium and caesium have shown an even stronger improvement of properties, leading to the highest certified efficiency to date (22.6%) for a cell with RbF PDT[1]. On the other hand Solar Frontier has recently announced measurements with an uncertified efficiency of 22.8% for cells with KF PDT at IW-CIGSTech 7. Further research in this direction, based on processes derived from PDT or new knowledge gained during investigation of its mechanism, will likely lead to new record efficiencies.

Compositional grading in the absorber layer

State-of-the-art CIGS thin film absorbers grown by co-evaporation generally show a varying indium to gallium ratio across their thickness. The relative amount of Ga determines the bandgap energy of CIGS, which can range from 1.0 eV for pure $CuInSe_2$ to 1.7 eV for pure $CuGaSe_2$, mainly due to a shift in the position of the conduction band maximum (CBM) [29]. Average bandgap energy values of 1.1-1.2 eV, corresponding to a [Ga]/([Ga]+[In]) ration of around 0.3 are used in record efficiency devices.

A Ga-grading profile was first introduced by Contreras et al. [30], and later extended as a consequence of the introduction of a three-stage deposition process by co-evaporation [31]. This process, which yields better crystallinity of the absorber layer, is based on the interdiffusion of the different elements, and naturally results in the formation a double grading profile with a higher Ga contents towards the front and the back interfaces, and lower Ga contents in the central-front region. This can be explained by a more favorable reaction between Cu and In than between Cu and Ga [32] and by different potential barriers for the diffusion of In and Ga through Cu vacancy defects [33]. As a consequence, there is a strong interplay between the amount of excess Cu supplied during the 3-stage process, the final overall amount of Cu, and the shape of Ga-grading profile [34,35]. Szaniawski et al. [36] reported that interpreting the effects of variations in the Cu content is complicated by the resulting variations in the Ga grading, which could explain the scarcity of studies on the effects of the Cu content in Ga-graded CIGS absorbers. The formation of the Ga grading

can also be influenced by other factors such as the presence and amount of alkalis during growth [37–39] and the deposition temperature [40]. The Ga grading resulting from a 3-stage process is typically further controlled by adjusting the In and Ga rates during CIGS growth [34,41].

One of the advantages of a Ga grading in CIGS absorbers is the presence of a back-surface field, which assists the drift of free electrons towards the front junction. This results in an improved collection of charge carriers, especially for photon energies in the near infrared [42]. Another advantage consists in the presence of a low-bandgap ("notch") region close to the front surface, enhancing the absorption of low-energy photons. Larger Ga content at the front interface of the absorber than in the notch ("front grading") is needed for improved junction quality. A small conduction band offset (< 0.3 eV) at the CdS/CIGS junction is reportedly beneficial for the interface quality, although a larger offset would result in a potential barrier for electrons and lead to increased interface recombination [43–45].

The ideal shape of the front and back gradings was investigated in depth by computer simulations, however without consensus being reached [33,46,47]. Experimental results reported in 2011 showed that an overly pronounced front grading can also result in a barrier for electrons, leading to enhanced recombination in the space-charged region [41]. To achieve a smoother front grading, the standard 3-stage process was modified into a multi-stage process, with the addition of several sub-stages in the evaporation rates of In and Ga [41]. Jackson et al. [12] reported on the other hand that an efficiency increase from 20.8% to 21.7% was partially achieved also thanks to a more pronounced front grading. This is however no contradiction, since the optimized Ga-grading profiles reported in [10] and [12] are similar in the front region of the absorber, as shown in Figure 2.

The technical complexity of a 3-stage process motivates investigations for simpler deposition methods. Salome [48] demonstrated in 2014 that, provided the implementation of a workable Ga-grading, a comparable absorber quality can be achieved on single-stage absorbers. The authors reported a small drop in efficiency from 17% of a 3-stage reference to 16.3% of the single-stage, which they attributed mainly to differences in the front surface grading. Mainz et al. [49] recently showed that recrystallization of the chalcopyrite phase during co-evaporation of CIS films might occur shortly before the segregation of Cu-Se on the surface. High-quality Cu-poor films could therefore be achieved without reaching a Cu-rich phase at all, which might open up the possibility of a passage to a much simpler and controllable process if the composition and crystal structure during the co-evaporation process is carefully in situ monitored. However, the study was performed on Ga-free absorbers and the eventual effect on the Ga grading is therefore unknown.

CIGS layers grown by a two-step process of selenization of a precursor have generally Ga accumulation at the back, near the Mo interface. Such a composition with a Ga depleted front surface is undesirable for high efficiency cells. Therefore precursor and selenization conditions are optimized for appropriately homogenized Ga concentration profile in two-step processed absorbers. However, for the highest efficiency solar cells an additional step of H_2S annealing is used to form a selenium rich CIGSSe layer in order to reach high V_{OC} values [50–52]. $CuInS_2$ and $CuGaS_2$ have a bandgap of 1.53 and 2.49 eV respectively, extending the systems range considerably. Contrary to Ga, the sulfur incorporation is mainly acting on the valence band minimum (VBM) [53]. Cells using partial sulfurization reach very high efficiencies, as for example the current efficiency record of Solar Frontier which most probably involves a sulfurization step. However full-sulfur CIGS (without any selenium) is still limited and reached 15.5% just recently [54].

Buffer layers

The following section focuses on the most recent advancements in buffer layers in CIGS solar cells since the review by Witte et al. [55]. For more details on the development and applications of buffer layers and transparent conducting oxides in CIGS cells the reader is referred to the extensive reviews by Naghavi et al. [17] and Hariskos et al. [56].

The highest conversion efficiencies in CIGS solar cells have been commonly achieved using chemical bath deposited (CBD) CdS as a buffer layer[9]. CdS seems to satisfy most requirements of a buffer layer with a suitable conduction band alignment to the absorber and the undoped ZnO and with a beneficial interface defect chemistry. It has been reported that positively charged Cd may form a stable donor-type defect in copper-deficient chalcopyrite surfaces resulting in an appropriate charge density and well defined Fermi-level position [57]. The major disadvantage of CdS is its relatively narrow band gap of about 2.4 eV leading to parasitic absorption losses to the cell current. Hence an extensive research on alternative buffer layers is ongoing, with Zn(S,O,OH), $Zn_{1-x}Mg_xO$, In_2S_3 and $Zn_{1-x}Sn_xO$ being the most promising materials to replace CdS so far. Solar frontier has done a pioneering development in the application of CBD grown Zn(S,O,OH) buffer layers and they use this process in their commercial production. Table 3 summarizes the champion devices based on the aforementioned buffer layers with their respective deposition methods, and Figure 3 highlights the current gains shown for some of those devices. The best conversion efficiency to date with an confirmed alternative buffer layer (Zn(S,O,OH)) is 21.0% [58] and was made possible by the combination with a new alkali PDT as discussed above, combined with a $Zn_{0.75}Mg_{0.25}O$/ZnO:Al window layer deposited by sputtering. The band gap of $ZnO_{1-x}S_x$ is tunable by varying the S/O ratio in between

3.2 eV (E_g, ZnO) and 3.6 eV (E_g, ZnS) with a bowing minimum close to 2.6 eV for x = 0.45 as reported by different groups [59–61]. Extensive optimization is often needed for an optimal band alignment to avoid metastabilities in the current-voltage measurements, requiring post-deposition treatments such as annealing and/or light soaking [62–64]. In the case of CBD, the similar solubility- and complex formation constants of ZnS, $Zn(OH)_2$ and ZnO, which were investigated i.e. by Hubert et al. [65], lead to a co-precipitation demanding for precise control of the deposition conditions. But even for atomic layer deposited (ALD) Zn(O,S), which is supposed to give the highest control over stoichiometry due to its layer-by-layer growth mode, post-deposition heat-light soaking effects have been reported [66]. The CBD method which currently leads to the highest power conversion efficiencies in CIGS/Zn(O,S) devices is based on "Zn^{2+}" and "S^{2-}" sources in a NH_3/H_2O medium at elevated temperatures. Current developments focus on faster reaction kinetics, i.e. deposition speed, by either exchanging the slowly de-composing thiourea, the established "S^{2-}"-source [67,68], or by the addition of additives [69] to satisfy the needs for an industrial application. For an all-vacuum process, sputter deposited Zn(O,S) achieved an efficiency of 18.3% [70]. Similar efficiencies have been reached with $Zn_{1-x}Mg_xO$ (18.1% [71]) and $Zn_{1-x}Sn_xO_y$ (18.2% [72]) buffer layers deposited by ALD. Indium sulfide is also among the most promising alternatives for CdS replacement. Using thermal evaporation an efficiency of 18.2% [73] has been achieved.

On sub-module scale an efficiency of 17.9% has been achieved recently on 30x30 cm^2, employing CBD-Zn(S,O,OH) [74]. The same sub-module efficiency was reached using a Indium sulfide [75] buffer layer.

Surface passivation

Charge carrier recombination at interfaces is still limiting the potential of CIGS solar cells. Concepts for surface passivation attempt to reduce recombination of diode and photocurrent at the absorber front and back interfaces. While the buffer already partly serves this function at the front, in this section we review the implementation of additional concepts such as structured and insulating passivation layers.

At the back contact interface of the CIGS solar cells, beside the back-surface field induced by the bandgap grading [77], passivation methods based on local point contacts were recently proposed [78], similar to those applied for high efficiency Si-based solar cells [79]. They could lead to improved cell properties especially for very thin or non-graded absorbers, where the grading alone is insufficient to prevent minority carrier recombination at the back contact. Alumina is one of the materials suggested for such applications. It reduces non-radiative recombination as a higher photoluminescence (PL) yield was observed for CIGS absorbers passivated with atomic

layer deposited Al_2O_3 [80,81]. Kotipalli et al. [82] found by CV measurements either positive or negative surface charge in or at the oxide/CIGS interface dependent on post deposition annealing conditions. SCAPS (Solar Cell Capacitance Simulator) [83] simulations by Vermang et al. [78] showed that the surface recombination velocity can be reduced from 10^4 - 10^6 cm s^{-1} to 10^2 - 10^3 cm s^{-1} for a CIGS device with local point contacts through an Al_2O_3 passivation layer at the back contact. In an experimental implementation of the idea, openings for local rear point contacts were achieved via e-beam lithography [84] or CdS particles [78]. A significant efficiency improvement for thin (< 1.6 um) ungraded absorbers has been observed. However, a beneficial effect of this back contact passivation approach for devices with a Ga grading towards the back contact has not been shown so far. Another effect of the structured or passivated back contacts is the possibility for better light management. Improvements in the efficiency for thin absorbers have recently been shown by different groups[85,86].

Front contact passivation can be approached in a similar manner to point contacts at the back. Simulations show possible performance improvements by choosing a suitable passivating material with appropriate point opening geometry [28,87–89]. Optimal point contact width and pitch were estimated to be in the 10 nm and 100 nm range respectively, based on current CIGS layer quality. Furthermore, for a good front contact passivation layer, donor-like defects close to the CBM of the CIGS (positive fixed charge) are preferred to increase the absorber surface inversion. [89]. Hultqvist et al. [90] have shown that ZnS can act as an effective passivation layer based on CV and PL measurements on metal-insulator-semiconductor type structures. Indeed, Allsop et al. [91] demonstrated experimentally that a thin layer of ZnS between the In_2S_3 buffer and CIGS absorber improves the solar cell performance. Subsequently, Fu et al. [92,93] have demonstrated a solar cell with point contacts to the buffer layer and a ZnS passivation layer from ZnS nanodots deposited by a spray-ILGAR method and Reinhard et al. [28] demonstrated the self-assembly of nano scale fluoride crystals on the absorber surface, which could serve as a template for passivation layer deposition.

Transparent contacts and stability behavior

Aluminum doped ZnO (AZO) is the most commonly applied transparent contact on CIGS and is mostly deposited by sputtering. Given the relatively low mobility (<30 cm^2 V^{-1} s^{-1}), AZO is heavily doped to achieve the necessary conductivity, leading to optical losses in the visible and NIR by free carrier absorption. This is especially problematic when using thick TCOs as required on a module level. Several alternative TCOs have been investigated to reduce free carrier absorption. An alternative, used by Solar Frontier, is chemical vapor deposited boron doped zinc oxide (BZO).

High mobilities up to 40 $cm^2 V^{-1} s^{-1}$ have been achieved with CIGS compatible deposition processes, while the carrier density is kept below ~$1*10^{20}$ cm^{-3} and therefore the TCO transparency and the short circuit current output is increased (Figure 4, left) [94]. Other recent works on high mobility TCOs for CIGS investigate nominally undoped ZnO, hydrogenated indium oxide (IOH) and indium zinc oxide (IZO) [95–98].

Investigations on the long term stability of CIGS modules have shown that the TCOs are strongly susceptible to degradation in humid atmosphere [99–103]. The conductivity of AZO degrades in humid atmosphere, which is caused by the chemisorption of environmental oxygen species, leading to zinc hydroxide and carbonate formation [104]. Chemisorption leads to the formation of potential barriers at grain boundaries, significantly reducing the mobility. Degradation in humid atmosphere is an intrinsic property of ZnO based TCO's and can only be diminished by increasing the layer density [105,106] or by applying proper encapsulation, which includes transparent front sheets with moisture barrier coatings, to prevent humidity exposure of the TCO [107]. Alternative TCO such as fluorine doped tin oxide (FTO), indium tin oxide (ITO) or indium zinc oxide (IZO) could also lead to considerable improvements in damp heat stability [108–110] (see Figure 4, right).

While sputtering or CVD are the most common deposition methods for the TCO, solution processed ZnO TCO's have been successfully applied on CIGS by chemical bath deposition [112], electrodeposition [113] and spray pyrolysis [114], but so far without meeting the performance and stability of sputtered reference cells. The major challenge for those processes lies in the fact that the deposition and/or subsequent annealing temperature should not exceed ~200°C at any process step[112].

State of the art efficiencies

Place Table 1 + Table 2 here

Concepts for high efficiency devices

Device concepts for achieving higher efficiency than in the single junction case include tandem (multi-junction) approaches and illumination under concentrated light. Such concepts for III-V solar cells are well developed, but their application for CIGS solar cells is still in an early stage. From an application point of view it is also interesting to improve the performance at low light irradiation and we will discuss this below.

Tandem solar cells

In order to reduce thermalization losses, or for better utilization of the solar spectrum, two or more solar cells of different bandgap are used in tandem solar cells as to reach higher photovoltaic conversion efficiency [146]. With ideally matched energy

bandgaps the theoretical conversion efficiency limit (detailed balance) under AM1.5G increases from ~33% for single junction to ~45% for dual junction solar cells [147]. Compared to single-crystalline waver based solar cells, where this concept has already been successfully applied, tandem devices based on all thin-film polycrystalline layers can profit from reduced complexity and therefore increased market potential. In this paragraph we review the current state of chalcogenide based all thin-film tandem devices. The bandgap variability in the chalcopyrite (CIGS) materials system opens an attractive option for tandem cells. For example CIS or CIGS cells with a bandgap of 1 to1.1 eV are suitable as a bottom cell in combination with a top cell of bandgap > 1.6-1.7 eV. Unfortunately CIGS cells with high bandgap suffer from poor electric properties and high sub bandgap absorption. Therefore, alternative absorbers such as DSSC, CdTe or perovskites have been applied as top cells [148–152] to investigate the feasibilities. The cells can be connected independently (4-terminal configuration, Figure 5) or in series (2-terminal configuration), while the later can be realized by monolithic cell interconnection or by string wise interconnection. An SEM cross-section of a 2-terminal monolithic tandem cell is shown in Figure 6. The best efficiencies published for this kind of device so far are 13.0% for a CIGS/DSSC [151] and 10.9% for a CIGS/Perovskite [150] device. While the 2-terminal concept has the advantages of reduced material usage, lower parasitic losses due to the reduced number of TCOs and the use of a single electric circuit it has the disadvantages of needing current matching between the sub cells, the requirement for a stable and efficient tunnel/recombination layer and the need for a bottom cell that's stable to the top cell deposition process.

While no efficiencies beyond the single junction record have been published so far, the improvements relative to the sub-cell properties shown in e.g. Figure 7 prove the validity of the concept [149,153,154] but obviously further research and development is needed.

Concentrator operation

Concentrator concepts have been shown in III-V solar cells very successfully [155]. CIGS solar cells are mainly considered for low concentrator applications, reaching 23.3% efficiency at 14.7 suns concentration so far [133]. Higher concentrations could be used when going for microcells, since both resistive losses and temperature increase are strongly reduced [156].

Low light behavior

Efficiency values for record devices are usually claimed for standard test conditions under AM1.5G illumination. However, good performance under low light conditions is also important to ensure lower levelized cost of electricity and for some other applica-

tions such as indoor energy generation. CIGS solar cell technology shows good performance under low light conditions compared to other technologies [4]. In Figure 8 we show the distribution of solar energy irradiated at different intensity levels on the example of Zuerich (Switzerland). The high fraction of energy received at low energy densities (more than 10% below 10 mW/cm^2) means that an efficiency reduction of only 10% under this irradiation can lead to total efficiency loss in the 1% range. Moreover, CIGS solar cells can also be used for indoor and portable electronics applications. Good performance under such conditions requires high parallel resistances (Rp) [157]. The curves in Figure 8 compare the efficiency of a device with Rp ~ 10 kΩ cm^2 (black) and Rp ~ 20 kΩ cm^2 (red). The resulting efficiency increase for light intensities below 1 mW/cm^2 is in the 50% (relative) range. This improvement would already lead to a change in annual power output from 177kWh/m^2 to 186 kWh/m^2 , which gives an increase of effective efficiency of 0.7% absolute (assuming a global irradiation of 1228 kWh and a distribution as given in Figure 8. The efficiency for each intensity level is averaged over the respective range and corrected for the spectral mismatch between AM1.5G and the LED test setup). The global irradiance for this experiment was measured in 10 minute intervals and the average distribution was obtained by evaluating a 10 year time series. The Low light efficiencies were measured under white LED irradiation and light levels were measured simultaneously with a thermopile sensor and a lux-meter.

The parallel resistance of CIGS solar cells has been reported to be influenced by localized hotspots [158,159], the window layer properties [157], the absorber composition, especially Cu content [160,161] and the laser scribing parameters [162–165]. These investigations show that CIGS solar cells can be optimized for efficient low light performance.

Flexible CIGS solar cell applications

CIGS thin film technology has been mostly developed on glass substrates, and for a long time CIGS solar cells deposited on flexible substrates such as plastic film or metal foil could not reach similar efficiencies. Limitations due to impurity diffusions or the need for lower growth temperature imposed by the choice of the substrate were reasons for such efficiency gap. Recent developments [7] however showed that those challenges can be overcome, and is best exemplified with an efficiency above 20% achieved on polyimide (PI) foil (see Table 1). Deposition on a flexible substrate has advantages not only for manufacturing (large area roll-to-roll deposition is possible), but opens up a whole new field for solar modules designs and applications. Especially, flexible and lightweight CIGS solar modules enable novel applications and concepts for solar electricity generation. Flexibility in shape, power rating, and form factor are some of the advantages that allow clear differentiation from traditional rigid

and heavy PV technology, opening the doors to BIPV and TIPV markets. Table 1 contains several companies which are active in this domain and offer this type of products or focus on mobile and fast-deployable off-grid solar solutions. As an example, Figure 9 shows potential products based on the module technology of Flisom AG. Beside full flexible solar modules, BIPV solutions can be provided by laminating lightweight solar modules directly onto metallic building elements. Significant reduction of BOS, transport and installation cost can be expected compared to conventional glass-glass technologies. In the following, we discuss in more detail two applications where lightweight is advantageous, namely space applications and tracking.

Space applications

Future satellite power subsystem will be designed to achieve higher power level, power densities (kW/kg), launch packaging densities (kW/m^3) and lower unit costs ($/kW) than can be achieved with current solar array technologies. Flexible CIGS solar cells offer the potential for providing very high power levels in a lightweight configuration that can be compactly packaged for launch.

For example, a 3 µm CIGS PV film (including front and back contact) grown on 25 µm polyimide substrate can achieve a specific power of ~4kW/kg (with a conversion efficiency of 15%). This value is potentially more than one order of magnitude above conventional solutions [166]. However, a polyimide substrate does not offer sufficient mechanical support for deployment, therefore a supporting back-sheet is needed. Further a front side encapsulation must be applied in order to protect against mechanical scratches and space environment. Both additional layers do significantly add up to the weight of the module. If relatively dense materials such as glass and steel are used as mechanical support, substrate or encapsulation respectively the specific power gets drastically reduced. In Table 4 some indicative numbers are summed up to give a range what specific power can be achieved in different configurations. The options of using a 50 µm fluorinated ethylene propylene FEP front laminate [167] or glass are included. If a carbon fiber reinforced plastic (CFRP) or titanium is used as lightweight support a power density of 0.3-0.5 kW/ kg seems achievable. If 100 µm steel is used as substrate and support the specific power drops to ~ 0.2 kW/kg. The estimation made here is consistent with the estimation of Dhere [168].

In terms of radiation hardness CIGS was found to be even superior to GaAs [169]. The bandgap of high efficiency (20%) flexible CIGS is around 1.1 eV [10]. However, a higher bandgap around 1.5 eV would not only be favorable to match the AM0 spectra but also to achieve a smaller temperature coefficient, as a module in space might reach temperatures up to ~150°C [169], but this has not yet been realized with com-

parable efficiency. A recent study confirmed the feasibility of the concept of a rollable blanket with integrated flexible CIGS submodules [170].

Tracking

Optimization of thin film solar modules for usage on PV trackers has lately re-appeared as a topic of interest in utility scale PV markets. First Solar announced during its Annual Analyst Day in 2016 [171], that its Series 5 module will be introduced to market in a three module configuration for fast installation in single axis tracker systems. This should contribute to reducing BOS costs of such systems significantly. The lightweight design of flexible solar modules has the additional advantage that the required tracker structures for utility PV systems could be considerably lighter and more cost effective. First concepts such as adaptive solar façade [172] or a moisture sensitive wooden-bilayers tracker [173] have been demonstrated employing light-weight modules.

Manufacturing technology

The transfer of the lab-scale processes into an industrial environment encounters challenges. Several aspects need to be controlled to ensure manufacturing of modules with acceptable efficiency and production yield. Not only material and process-related issues need to be solved, but also engineering of new equipment machines and development of in-situ process control techniques are required. Industrial production of CIGS solar modules on glass substrates has advanced to high volumes by companies such as Solar Frontier, AVANCIS, Solibro, Manz and others. However the manufacturing of flexible CIGS solar cells and modules is relatively less mature despite decent cell efficiencies have been achieved on small area devices in labs (see Table 1 and 2). Flexible substrates allow the use of roll-to-roll deposition techniques, as used in the packaging industry, with the potential advantage of high throughput and compact equipment dimensions for each layer of the solar module stack. For the CIGS absorber deposition by co-evaporation or sputtering, evaporation sources and targets need to be positioned in such a way as to reproduce the CIGS growth conditions from the static processes developed on laboratory scale. Adequate in-situ process control techniques are necessary to ensure stable absorber quality during the continuous deposition onto the moving substrate. As there is a lack of reliable providers for CIGS roll-to-roll deposition equipment, companies such as Flisom have developed custom solutions.

Figure 10 shows I-V and EQE curve of a 16.0% solar cell based on a CIGS absorber grown by roll-to-roll low-temperature co-evaporation onto a flexible polyimide foil. The best corresponding mini-module (5x5 cm^2, 8 cells monolithically connected by laser scribing) achieved an efficiency of 14.3%. The SEM cross-section shows an absorber

microstructure with large grains, with a TCO deposited in a R2R process. Further improvements, not only of CIGS growth conditions but in overall stack and module design, are still required to reach similar efficiency values as reported on laboratory-scale for a similar process (e.g. 16.9% for monolithic CIGS on PI [25]). Those results, together with results reported on stainless steel (e.g. MiaSolé with 16.5% efficiency [123] and Global Solar with 14.7% (presented at IW-CIGSTech 7) on module size or 17 % on 6'' cells from Midsummer [124]) show that module manufacturing on flexible substrate is on a good path to be cost-competitive in a near future.

Conclusions and prospects

The application of alkali PDT by several labs around the world has been one of the main trigger for the quick progress of record efficiencies observed over the past couple of years. Alternative buffer layers, especially based on Zn(O,OH,S) and TCOs have yielded remarkably high efficiency and stable performance.

It will however take some time to fully translate those new developments into industrial production. Considering the significant and fast improvements observed on lab-scale, it is likely that this new knowledge will contribute greatly in increasing the performance of industrial CIGS modules in the near future. Moreover, the large scale production of solar modules on flexible substrate gives the opportunity for differentiated products, applicable where traditional rigid heavy modules have some limitations. Flexible lightweight solar modules will find their application and growth, especially for BIPV.

The combination of CIGS with wide bandgap perovskite shows interesting options for tandem solar cells, however further research is needed to enhance device efficiency. CIGS solar cell processing can further be optimized, for example to enhance parallel resistance in order to make them more efficient in low light applications.

Acknowledgements

This work was partially supported by the Swiss State Secretariat for Education, Research and Innovation (SERI) under contract number REF-1131-52107, the National Research Programm "Energy Turnaround" (NRP 70) of the Swiss National Science Foundation (SNSF) in the project PV2050, the Swiss National Science Foundation (grant number 20NA21_150950 and 200021_149453/1), the Swiss Federal Office of Energy (grant number SI/501145-01 and SI/501072-01), and the Competence Center for Energy & Mobility (CCEM) project 906_CONNECT PV.

The authors would like to acknowledge the Swiss National Air Pollution Monitoring Network NABEL (BAFU and Empa) for the global irradiation data.

References

1 Jackson P, Wuerz R, Hariskos D, Lotter E, Witte W, Powalla M. Effects of heavy alkali elements in Cu(In,Ga)Se2 solar cells with efficiencies up to 22.6%. *physica status solidi (RRL) – Rapid Research Letters* 2016: n/a-n/a. DOI: 10.1002/pssr.201600199.

2 Makrides G, Zinsser B, Norton M, Georghiou GE, Schubert M, Werner JH. Potential of photovoltaic systems in countries with high solar irradiation. *Renewable and Sustainable Energy Reviews* 2010; **14**(2): 754–762. DOI: 10.1016/j.rser.2009.07.021.

3 Bhandari KP, Collier JM, Ellingson RJ, Apul DS. Energy payback time (EPBT) and energy return on energy invested (EROI) of solar photovoltaic systems: A systematic review and meta-analysis. *Renewable and Sustainable Energy Reviews* 2015; **47**: 133–141. DOI: 10.1016/j.rser.2015.02.057.

4 CIS advantages in real-world conditions.Solar Frontier company webpageAccesed May 23, 2016http://www.solar-frontier.com/eng/technology/Performance/index.html.

5 CIGS White Paper Initiative – CIGS Thin-Film Photovoltaics.CIGS White Paper InitiativeAccesed May 14, 2016http://cigs-pv.net/cigs-white-paper-initiative/.

6 Otte K, Makhova L, Braun A, Konovalov I. Flexible Cu(In,Ga)Se2 thin-film solar cells for space application. *Thin Solid Films* 2006; **511–512**: 613–622. DOI: 10.1016/j.tsf.2005.11.068.

7 Reinhard P, Chirilă A, Blösch P, Pianezzi F, Nishiwaki S, Buecheler S, Tiwari AN. Review of Progress Toward 20% Efficiency Flexible CIGS Solar Cells and Manufacturing Issues of Solar Modules. *IEEE Journal of Photovoltaics* 2013; **3**(1): 572–580. DOI: 10.1109/JPHOTOV.2012.2226869.

8 Shafarman WN, Siebentritt S, Stolt L. Cu(InGa)Se2 Solar Cells. In *Handbook of Photovoltaic Science and Engineering*, Luque A, Hegedus S (eds). John Wiley & Sons, Ltd, 2010; 546–599.

9 Roland Scheer, Hans-Werner Schock. *Chalcogenide Photovoltaics: Physics, Technologies, and Thin Film Devices*. Wiley, 2011.

10 Chirilă A, Reinhard P, Pianezzi F, Bloesch P, Uhl AR, Fella C, Kranz L, Keller D, Gretener C, Hagendorfer H, Jaeger D, Erni R, Nishiwaki S, Buecheler S, Tiwari AN. Potassium-induced surface modification of Cu(In,Ga)Se2 thin films for high-efficiency solar cells. *Nature Materials* 2013; **12**(12): 1107–1111. DOI: 10.1038/nmat3789.

11 NREL: National Center for Photovoltaics Home Page.Accesed April 27, 2016http://www.nrel.gov/ncpv/.

12 Jackson P, Hariskos D, Wuerz R, Kiowski O, Bauer A, Friedlmeier TM, Powalla M. Properties of Cu(In,Ga)Se2 solar cells with new record efficiencies up to

21.7%. *physica status solidi (RRL) – Rapid Research Letters* 2015; **9**(1): 28–31. DOI: 10.1002/pssr.201409520.

13 Kushiya K. CIS-based thin-film PV technology in solar frontier K.K. *Solar Energy Materials and Solar Cells* 2014; **122**: 309–313. DOI: 10.1016/j.solmat.2013.09.014.

14 Solar Frontier Achieves World Record Thin-Film Solar Cell Efficiency: 22.3%.Solar Frontier company webpageDecember 8, 2015Accesed April 25, 2016http://www.solar-frontier.com/eng/news/2015/C051171.html.

15 Fortunato E, Ginley D, Hosono H, Paine DC. Transparent Conducting Oxides for Photovoltaics. *MRS Bulletin* 2007; **32**(3): 242–247. DOI: 10.1557/mrs2007.29.

16 Rau U, Grabitz PO, Werner JH. Resistive limitations to spatially inhomogeneous electronic losses in solar cells. *Applied Physics Letters* 2004; **85**(24): 6010–6012. DOI: 10.1063/1.1835536.

17 Naghavi N, Abou-Ras D, Allsop N, Barreau N, Bücheler S, Ennaoui A, Fischer C-H, Guillen C, Hariskos D, Herrero J, Klenk R, Kushiya K, Lincot D, Menner R, Nakada T, Platzer-Björkman C, Spiering S, Tiwari AN, Törndahl T. Buffer layers and transparent conducting oxides for chalcopyrite Cu(In,Ga)(S,Se)2 based thin film photovoltaics: present status and current developments. *Progress in Photovoltaics: Research and Applications* 2010; **18**(6): 411–433. DOI: 10.1002/pip.955.

18 Hedstrom J, Ohlsen H, Bodegard M, Kylner A, Stolt L, Hariskos D, Ruckh M, Schock HW. Zno/Cds/Cu(in,Ga)Se2 Thin-Film Solar-Cells with Improved Performance. *Conference Record of the Twenty Third Ieee Photovoltaic Specialists Conference - 1993* 1993: 364–371. DOI: 10.1109/Pvsc.1993.347154.

19 Rudmann D, Brémaud D, da Cunha AF, Bilger G, Strohm A, Kaelin M, Zogg H, Tiwari AN. Sodium incorporation strategies for CIGS growth at different temperatures. *Thin Solid Films* 2005; **480–481**: 55–60. DOI: 10.1016/j.tsf.2004.11.071.

20 Rudmann D, da Cunha AF, Kaelin M, Kurdesau F, Zogg H, Tiwari AN, Bilger G. Efficiency enhancement of Cu(In,Ga)Se_2 solar cells due to post-deposition Na incorporation. *Applied Physics Letters* 2004; **84**(7): 1129–1131. DOI: doi:10.1063/1.1646758.

21 Reinhard P, Bissig B, Pianezzi F, Avancini E, Hagendorfer H, Keller D, Fuchs P, Döbeli M, Vigo C, Crivelli P, Nishiwaki S, Buecheler S, Tiwari AN. Features of KF and NaF Postdeposition Treatments of Cu(In,Ga)Se2 Absorbers for High Efficiency Thin Film Solar Cells. *Chemistry of Materials* 2015. DOI: 10.1021/acs.chemmater.5b02335.

22 Mansfield LM, Noufi R, Muzzillo CP, DeHart C, Bowers K, To B, Pankow JW, Reedy RC, Ramanathan K. Enhanced Performance in Cu(In,Ga)Se Solar Cells Fabricated by the Two-Step Selenization Process With a Potassium Fluoride Postdeposition Treatment. *IEEE Journal of Photovoltaics* 2014; **4**(6): 1650–1654. DOI: 10.1109/JPHOTOV.2014.2354259.

23 Laemmle A, Wuerz R, Powalla M. Efficiency enhancement of Cu(In,Ga)Se2 thin-film solar cells by a post-deposition treatment with potassium fluoride. *physica*

status solidi (RRL) – Rapid Research Letters 2013; **7**(9): 631–634. DOI: 10.1002/pssr.201307238.

24 Jackson P, Hariskos D, Wuerz R, Kiowski O, Bauer A, Powalla M. Properties of high efficiency Cu (In, Ga) Se2 solar cells. In *MRS Spring Meeting & Exhibit, San Francisco B*, vol 7, 2015.

25 Reinhard P, Pianezzi F, Bissig B, Chirila A, Blosch P, Nishiwaki S, Buecheler S, Tiwari AN. Cu(In,Ga)Se Thin-Film Solar Cells and Modules - A Boost in Efficiency Due to Potassium. *IEEE Journal of Photovoltaics* 2015; **5**(2): 656–663. DOI: 10.1109/JPHOTOV.2014.2377516.

26 Jackson P, Hariskos D, Wuerz R, Wischmann W, Powalla M. Compositional investigation of potassium doped Cu(In,Ga)Se2 solar cells with efficiencies up to 20.8%. *physica status solidi (RRL) – Rapid Research Letters* 2014; **8**(3): 219–222. DOI: 10.1002/pssr.201409040.

27 Herrmann D, Kratzert P, Weeke S, Zimmer M, Djordjevic-Reiss J, Hunger R, Lindberg P, Wallin E, Lundberg O, Stolt L. CIGS module manufacturing with high deposition rates and efficiencies. In *2014 IEEE 40th Photovoltaic Specialist Conference (PVSC)*, 2014; 2775–2777. DOI: 10.1109/PVSC.2014.6925505.

28 Reinhard P, Bissig B, Pianezzi F, Hagendorfer H, Sozzi G, Menozzi R, Gretener C, Nishiwaki S, Buecheler S, Tiwari AN. Alkali-Templated Surface Nanopatterning of Chalcogenide Thin Films: A Novel Approach Toward Solar Cells with Enhanced Efficiency. *Nano Letters* 2015; **15**(5): 3334–3340. DOI: 10.1021/acs.nanolett.5b00584.

29 Wei S-H, Zhang SB, Zunger A. Effects of Na on the electrical and structural properties of CuInSe2. *Journal of Applied Physics* 1999; **85**(10): 7214–7218. DOI: 10.1063/1.370534.

30 Contreras M, Tuttle J, Du D, Qi Y, Swartzlander A, Tennant A, Noufi R. Graded band-gap Cu(In,Ga)Se2 thin-film solar cell absorber with enhanced open-circuit voltage. *Applied Physics Letters* 1993; **63**(13): 1824–1826. DOI: 10.1063/1.110675.

31 Gabor AM, Tuttle JR, Albin DS, Contreras MA, Noufi R, Hermann AM. High-efficiency CuInxGa1−xSe2 solar cells made from (Inx,Ga1−x)2Se3 precursor films. *Applied Physics Letters* 1994; **65**(2): 198–200. DOI: 10.1063/1.112670.

32 Marudachalam M, Birkmire RW, Hichri H, Schultz JM, Swartzlander A, Al-Jassim MM. Phases, morphology, and diffusion in CuInxGa1−xSe2 thin films. *Journal of Applied Physics* 1997; **82**(6): 2896–2905. DOI: 10.1063/1.366122.

33 Witte W, Abou-Ras D, Albe K, Bauer GH, Bertram F, Boit C, Brüggemann R, Christen J, Dietrich J, Eicke A, Hariskos D, Maiberg M, Mainz R, Meessen M, Müller M, Neumann O, Orgis T, Paetel S, Pohl J, Rodriguez-Alvarez H, Scheer R, Schock H-W, Unold T, Weber A, Powalla M. Gallium gradients in Cu(In,Ga)Se2 thin-film solar cells. *Progress in Photovoltaics: Research and Applications* 2015; **23**(6): 717–733. DOI: 10.1002/pip.2485.

34 Seyrling S, Chirila A, Güttler D, Pianezzi F, Rossbach P, Tiwari AN. Modification of the three-stage evaporation process for CuIn1−xGaxSe2 absorber deposition. *Thin Solid Films* 2011; **519**(21): 7232–7236. DOI: 10.1016/j.tsf.2010.12.146.

35 Reinhard P, Pianezzi F, Kranz L, Nishiwaki S, Chirilă A, Buecheler S, Tiwari AN. Flexible Cu(In,Ga)Se2 solar cells with reduced absorber thickness. *Progress in Photovoltaics: Research and Applications* 2015; **23**(3): 281–289. DOI: 10.1002/pip.2420.

36 Szaniawski P, Salomé P, Fjällström V, Törndahl T, Zimmermann U, Edoff M. Influence of Varying Cu Content on Growth and Performance of Ga-Graded Cu(In,Ga)Se2 Solar Cells. *IEEE Journal of Photovoltaics* 2015; **5**(6): 1775–1782. DOI: 10.1109/JPHOTOV.2015.2478033.

37 Bissig B, Reinhard P, Pianezzi F, Hagendorfer H, Nishiwaki S, Buecheler S, Tiwari AN. Effects of NaF evaporation during low temperature Cu(In,Ga)Se2 growth. *Thin Solid Films* 2015; **582**: 56–59. DOI: 10.1016/j.tsf.2014.11.026.

38 Salomé PMP, Rodriguez-Alvarez H, Sadewasser S. Incorporation of alkali metals in chalcogenide solar cells. *Solar Energy Materials and Solar Cells* 2015; **143**: 9–20. DOI: 10.1016/j.solmat.2015.06.011.

39 Rudmann D, Brémaud D, Zogg H, Tiwari AN. Na incorporation into Cu(In,Ga)Se2 for high-efficiency flexible solar cells on polymer foils. *Journal of Applied Physics* 2005; **97**(8): 84903. DOI: 10.1063/1.1857059.

40 Nishiwaki S, Satoh T, Hashimoto Y, Negami T, Wada T. Preparation of Cu(In,Ga)Se2 thin films at low substrate temperatures. *Journal of Materials Research* 2001; **16**(2): 394–399. DOI: 10.1557/JMR.2001.0059.

41 Chirilă A, Buecheler S, Pianezzi F, Bloesch P, Gretener C, Uhl AR, Fella C, Kranz L, Perrenoud J, Seyrling S, Verma R, Nishiwaki S, Romanyuk YE, Bilger G, Tiwari AN. Highly efficient Cu(In,Ga)Se2 solar cells grown on flexible polymer films. *Nature Materials* 2011; **10**(11): 857–861. DOI: 10.1038/nmat3122.

42 Dullweber T, anna GH, Rau U, Schock HW. A new approach to high-efficiency solar cells by band gap grading in Cu(In,Ga)Se2 chalcopyrite semiconductors. *Solar Energy Materials and Solar Cells* 2001; **67**(1–4): 145–150. DOI: 10.1016/S0927-0248(00)00274-9.

43 Niemegeers A, Burgelman M, Herberholz R, Rau U, Hariskos D, Schock H-W. Model for electronic transport in Cu(In,Ga)Se2 solar cells. *Progress in Photovoltaics: Research and Applications* 1998; **6**(6): 407–421. DOI: 10.1002/(SICI)1099-159X(199811/12)6:6<407::AID-PIP230>3.0.CO;2-U.

44 Klenk R. Characterisation and modelling of chalcopyrite solar cells. *Thin Solid Films* 2001; **387**(1–2): 135–140. DOI: 10.1016/S0040-6090(00)01736-3.

45 Sozzi G, Troni F, Menozzi R. On the combined effects of window/buffer and buffer/absorber conduction-band offsets, buffer thickness and doping on thin-film solar cell performance. *Solar Energy Materials and Solar Cells* 2014; **121**: 126–136. DOI: 10.1016/j.solmat.2013.10.037.

46 Gloeckler M, Sites JR. Band-gap grading in Cu(In,Ga)Se2 solar cells. *Journal of Physics and Chemistry of Solids* 2005; **66**(11): 1891–1894. DOI: 10.1016/j.jpcs.2005.09.087.

47 Decock K, Khelifi S, Burgelman M. Analytical versus numerical analysis of back grading in CIGS solar cells. *Solar Energy Materials and Solar Cells* 2011; **95**(6): 1550–1554. DOI: 10.1016/j.solmat.2010.10.020.

48 Salomé PMP, Fjällström V, Szaniawski P, Leitão JP, Hultqvist A, Fernandes PA, Teixeira JP, Falcão BP, Zimmermann U, da Cunha AF, Edoff M. A comparison between thin film solar cells made from co-evaporated CuIn1-xGaxSe2 using a one-stage process versus a three-stage process. *Progress in Photovoltaics: Research and Applications* 2015; **23**(4): 470–478. DOI: 10.1002/pip.2453.

49 Mainz R, Rodriguez-Alvarez H, Klaus M, Thomas D, Lauche J, Weber A, Heinemann MD, Brunken S, Greiner D, Kaufmann CA, Unold T, Schock H-W, Genzel C. Sudden stress relaxation in compound semiconductor thin films triggered by secondary phase segregation. *Physical Review B* 2015; **92**(15): 155310. DOI: 10.1103/PhysRevB.92.155310.

50 Nakada T, Ohbo H, Watanabe T, Nakazawa H, Matsui M, Kunioka A. Improved Cu(In,Ga)(S,Se)2 thin film solar cells by surface sulfurization. *Solar Energy Materials and Solar Cells* 1997; **49**(1–4): 285–290. DOI: 10.1016/S0927-0248(97)00054-8.

51 Ohashi D, Nakada T, Kunioka A. Improved CIGS thin-film solar cells by surface sulfurization using In2S3 and sulfur vapor. *Solar Energy Materials and Solar Cells* 2001; **67**(1–4): 261–265. DOI: 10.1016/S0927-0248(00)00290-7.

52 Lavrenko T, Ott T, Walter T. Impact of sulfur and gallium gradients on the performance of thin film Cu(In,Ga)(Se,S)2 solar cells. *Thin Solid Films* 2015; **582**: 51–55. DOI: 10.1016/j.tsf.2014.11.024.

53 Kobayashi T, Yamaguchi H, Jehl Li Kao Z, Sugimoto H, Kato T, Hakuma H, Nakada T. Impacts of surface sulfurization on Cu(In1−x,Gax)Se2 thin-film solar cells. *Progress in Photovoltaics: Research and Applications* 2015; **23**(10): 1367–1374. DOI: 10.1002/pip.2554.

54 Hiroi H, Iwata Y, Adachi S, Sugimoto H, Yamada A. New World-Record Efficiency for Pure-Sulfide Cu(In,Ga)S2 Thin-Film Solar Cell With Cd-Free Buffer Layer via KCN-Free Process. *IEEE Journal of Photovoltaics* 2016; **6**(3): 760–763. DOI: 10.1109/JPHOTOV.2016.2537540.

55 Witte W, Spiering S, Hariskos D. Substitution of the CdS buffer layer in CIGS thin-film solar cells. *Vakuum in Forschung und Praxis* 2014; **26**(1): 23–27. DOI: 10.1002/vipr.201400546.

56 Hariskos D, Spiering S, Powalla M. Buffer layers in Cu(In,Ga)Se2 solar cells and modules. *Thin Solid Films* 2005; **480–481**: 99–109. DOI: 10.1016/j.tsf.2004.11.118.

57 Wada T, Hayashi S, Hashimoto Y, Nishiwaki S, Sato T, Negami T, Nishitani M. High efficiency Cu (In, Ga) Se2 (CIGS) solar cells with improved CIGS surface. In

Proceedings of the 2nd World Conference and Exhibition on Photovoltaic Energy Conversion, 1998; 403–408.

58 Friedlmeier TM, Jackson P, Bauer A, Hariskos D, Kiowski O, Wuerz R, Powalla M. Improved Photocurrent in Cu(In,Ga)Se2 Solar Cells: From 20.8 % to 21.7 % Efficiency with CdS Buffer and 21.0 % Cd-Free. *IEEE Journal of Photovoltaics* 2015; **5**(5): 1487–1491. DOI: 10.1109/JPHOTOV.2015.2458039.

59 Meyer BK, Polity A, Farangis B, He Y, Hasselkamp D, Krämer T, Wang C. Structural properties and bandgap bowing of ZnO1−xSx thin films deposited by reactive sputtering. *Applied Physics Letters* 2004; **85**(21): 4929–4931. DOI: 10.1063/1.1825053.

60 Persson C, Platzer-Björkman C, Malmström J, Törndahl T, Edoff M. Strong Valence-Band Offset Bowing of ZnO(1-x)Sx Enhances p-Type Nitrogen Doping of ZnO-like Alloys. *Physical Review Letters* 2006; **97**(14): 146403. DOI: 10.1103/PhysRevLett.97.146403.

61 Grimm A, Kieven D, Klenk R, Lauermann I, Neisser A, Niesen T, Palm J. Junction formation in chalcopyrite solar cells by sputtered wide gap compound semiconductors. *Thin Solid Films* 2011; **520**(4): 1330–1333. DOI: 10.1016/j.tsf.2011.04.150.

62 Naghavi N, Temgoua S, Hildebrandt T, Guillemoles JF, Lincot D. Impact of oxygen concentration during the deposition of window layers on lowering the metastability effects in Cu(In,Ga)Se2/CBD Zn(S,O) based solar cell. *Progress in Photovoltaics: Research and Applications* 2015; **23**(12): 1820–1827. DOI: 10.1002/pip.2626.

63 Buffière M, Barreau N, Arzel L, Zabierowski P, Kessler J. Minimizing metastabilities in Cu(In,Ga)Se2/(CBD)Zn(S,O,OH)/i-ZnO-based solar cells. *Progress in Photovoltaics: Research and Applications* 2015; **23**(4): 462–469. DOI: 10.1002/pip.2451.

64 Kobayashi T, Kumazawa T, Jehl Li Kao Z, Nakada T. Post-treatment effects on ZnS(O,OH)/Cu(In,Ga)Se2 solar cells deposited using thioacetamide-ammonia based solution. *Solar Energy Materials and Solar Cells* 2014; **123**: 197–202. DOI: 10.1016/j.solmat.2014.01.013.

65 Hubert C, Naghavi N, Canava B, Etcheberry A, Lincot D. Thermodynamic and experimental study of chemical bath deposition of Zn(S,O,OH) buffer layers in basic aqueous ammonia solutions. Cell results with electrodeposited CuIn(S,Se)2 absorbers. *Thin Solid Films* 2007; **515**(15): 6032–6035. DOI: 10.1016/j.tsf.2006.12.139.

66 Kobayashi T, Kao ZJL, Nakada T. Temperature dependent current–voltage and admittance spectroscopy on heat-light soaking effects of Cu(In,Ga)Se2 solar cells with ALD-Zn(O,S) and CBD-ZnS(O,OH) buffer layers. *Solar Energy Materials and Solar Cells* 2015; **143**: 159–167. DOI: 10.1016/j.solmat.2015.06.044.

67 Hariskos D, Menner R, Jackson P, Paetel S, Witte W, Wischmann W, Powalla M, Bürkert L, Kolb T, Oertel M, Dimmler B, Fuchs B. New reaction kinetics for a high-rate chemical bath deposition of the Zn(S,O) buffer layer for Cu(In,Ga)Se2-based

solar cells. *Progress in Photovoltaics: Research and Applications* 2012; **20**(5): 534–542. DOI: 10.1002/pip.1244.

68 Löckinger J, Nishiwaki S, Fuchs P, Buecheler S, Romanyuk YE, Tiwari AN. New sulphide precursors for Zn(O,S) buffer layers in Cu(In,Ga)Se2 solar cells for faster reaction kinetics. *Journal of Optics* 2016; **18**(8): 84002. DOI: 10.1088/2040-8978/18/8/084002.

69 Hildebrandt T, Loones N, Bouttemy M, Vigneron J, Etcheberry A, Lincot D, Naghavi N. Toward a Better Understanding of the Use of Additives in Zn(S,O) Deposition Bath for High-Efficiency Cu(In,Ga)Se2-Based Solar Cells. *IEEE Journal of Photovoltaics* 2015; **5**(6): 1821–1826. DOI: 10.1109/JPHOTOV.2015.2478066.

70 Klenk R, Steigert A, Rissom T, Greiner D, Kaufmann CA, Unold T, Lux-Steiner MC. Junction formation by Zn(O,S) sputtering yields CIGSe-based cells with efficiencies exceeding 18%. *Progress in Photovoltaics: Research and Applications* 2014; **22**(2): 161–165. DOI: 10.1002/pip.2445.

71 Törndahl T, Hultqvist A, Platzer-Björkman C, Edoff M. Growth and characterization of ZnO-based buffer layers for CIGS solar cells. In vol 7603, 2010; 76030D–76030D–9. DOI: 10.1117/12.846351.

72 Lindahl J, Zimmermann U, Szaniawski P, Törndahl T, Hultqvist A, Salomé P, Platzer-Björkman C, Edoff M. Inline Cu(In,Ga)Se Co-evaporation for High-Efficiency Solar Cells and Modules. *IEEE Journal of Photovoltaics* 2013; **3**(3): 1100–1105. DOI: 10.1109/JPHOTOV.2013.2256232.

73 Spiering S, Nowitzki A, Kessler F, Igalson M, Abdel Maksoud H. Optimization of buffer-window layer system for CIGS thin film devices with indium sulphide buffer by in-line evaporation. *Solar Energy Materials and Solar Cells* 2016; **144**: 544–550. DOI: 10.1016/j.solmat.2015.09.038.

74 Nam J, Kang Y, Lee D, Yang J, Kim Y-S, Mo CB, Park S, Kim D. Achievement of 17.9% efficiency in 30 × 30 cm2 Cu(In,Ga)(Se,S)2 solar cell sub-module by sulfurization after selenization with Cd-free buffer. *Progress in Photovoltaics: Research and Applications* 2016; **24**(2): 175–182. DOI: 10.1002/pip.2653.

75 AVANCIS erzielt erneuten Wirkungsgradrekord: Fraunhofer ISE zertifiziert CIGS-Solarmodul mit Wirkungsgrad von 17,9 %.AVANCIS Advanced Solar PowerMay 2, 2016Accesed May 9, 2016http://www.avancis.de/footer/presse/newsansicht/article/avancis-erzielt-erneuten-wirkungsgradrekord-fraunhofer-ise-zertifiziert-cigs-solarmodul-mit-wirkungsgrad-von-179.html.

76 Kobayashi T, Jehl Li Kao Z, Kato T, Sugimoto H, Nakada T. A comparative study of Cd- and Zn-compound buffer layers on Cu(In1−x,Gax)(Sy,Se1−y)2 thin film solar cells. *Progress in Photovoltaics: Research and Applications* 2016; **24**(3): 389–396. DOI: 10.1002/pip.2695.

77 Lundberg O, Edoff M, Stolt L. The effect of Ga-grading in CIGS thin film solar cells. *Thin Solid Films* 2005; **480–481**: 520–525. DOI: 10.1016/j.tsf.2004.11.080.

78 Vermang B, Fjällström V, Pettersson J, Salomé P, Edoff M. Development of rear surface passivated Cu(In,Ga)Se2 thin film solar cells with nano-sized local rear point contacts. *Solar Energy Materials and Solar Cells* 2013; **117**: 505–511. DOI: 10.1016/j.solmat.2013.07.025.

79 Blakers AW, Wang A, Milne AM, Zhao J, Green MA. 22.8% efficient silicon solar cell. *Applied Physics Letters* 1989; **55**(13): 1363–1365. DOI: 10.1063/1.101596.

80 Hsu W-W, Chen JY, Cheng T-H, Lu SC, Ho W-S, Chen Y-Y, Chien Y-J, Liu CW. Surface passivation of Cu(In,Ga)Se2 using atomic layer deposited Al2O3. *Applied Physics Letters* 2012; **100**(2): 23508. DOI: 10.1063/1.3675849.

81 Joel J, Vermang B, Larsen J, Donzel-Gargand O, Edoff M. On the assessment of CIGS surface passivation by photoluminescence. *physica status solidi (RRL) – Rapid Research Letters* 2015; **9**(5): 288–292. DOI: 10.1002/pssr.201510081.

82 Kotipalli R, Vermang B, Joel J, Rajkumar R, Edoff M, Flandre D. Investigating the electronic properties of Al2O3/Cu(In,Ga)Se2 interface. *AIP Advances* 2015; **5**(10): 107101. DOI: 10.1063/1.4932512.

83 Burgelman M, Nollet P, Degrave S. Modelling polycrystalline semiconductor solar cells. *Thin Solid Films* 2000; **361–362**: 527–532. DOI: 10.1016/S0040-6090(99)00825-1.

84 Vermang B, Wätjen JT, Frisk C, Fjällström V, Rostvall F, Edoff M, Salomé P, Borme J, Nicoara N, Sadewasser S. Introduction of Si PERC Rear Contacting Design to Boost Efficiency of Cu(In,Ga)Se Solar Cells. *IEEE Journal of Photovoltaics* 2014; **4**(6): 1644–1649. DOI: 10.1109/JPHOTOV.2014.2350696.

85 Vermang B, Wätjen JT, Fjällström V, Rostvall F, Edoff M, Gunnarsson R, Pilch I, Helmersson U, Kotipalli R, Henry F, Flandre D. Highly reflective rear surface passivation design for ultra-thin Cu(In,Ga)Se2 solar cells. *Thin Solid Films* 2015; **582**: 300–303. DOI: 10.1016/j.tsf.2014.10.050.

86 van Lare C, Yin G, Polman A, Schmid M. Light Coupling and Trapping in Ultrathin Cu(In,Ga)Se2 Solar Cells Using Dielectric Scattering Patterns. *ACS Nano* 2015; **9**(10): 9603–9613. DOI: 10.1021/acsnano.5b04091.

87 Allsop N, Nürnberg R, Lux-Steiner MC, Schedel-Niedrig T. Three-dimensional simulations of a thin film heterojunction solar cell with a point contact/defect passivation structure at the heterointerface. *Applied Physics Letters* 2009; **95**(12): 122108. DOI: 10.1063/1.3233962.

88 Sozzi G, Pignoloni D, Menozzi R, Pianezzi F, Reinhard P, Bissig B, Buecheler S, Tiwari AN. Designing CIGS solar cells with front-side point contacts. In *Photovoltaic Specialist Conference (PVSC), 2015 IEEE 42nd*, 2015; 1–5. DOI: 10.1109/PVSC.2015.7355691.

89 Bercegol A, Chacko B, Klenk R, Lauermann I, Lux-Steiner MC, Liero M. Point contacts at the copper-indium-gallium-selenide interface—A theoretical outlook. *Journal of Applied Physics* 2016; **119**(15): 155304. DOI: 10.1063/1.4947267.

90 Hultqvist A, Li JV, Kuciauskas D, Dippo P, Contreras MA, Levi DH, Bent SF. Reducing interface recombination for Cu(In,Ga)Se2 by atomic layer deposited buffer layers. *Applied Physics Letters* 2015; **107**(3): 33906. DOI: 10.1063/1.4927096.

91 Allsop NA, Camus C, Hänsel A, Gledhill SE, Lauermann I, Lux-Steiner MC, Fischer C-H. Indium sulfide buffer/CIGSSe interface engineering: Improved cell performance by the addition of zinc sulfide. *Thin Solid Films* 2007; **515**(15): 6068–6072. DOI: 10.1016/j.tsf.2006.12.084.

92 Fu Y, Allsop NA, Gledhill SE, Köhler T, Krüger M, Sáez-Araoz R, Blöck U, Lux-Steiner MC, Fischer C-H. ZnS Nanodot Film as Defect Passivation Layer for Cu(In,Ga)(S,Se)2 Thin-Film Solar Cells Deposited by Spray-ILGAR (Ion-Layer Gas Reaction). *Advanced Energy Materials* 2011; **1**(4): 561–564. DOI: 10.1002/aenm.201100146.

93 Fu Y, Sáez-Araoz R, Köhler T, Krüger M, Steigert A, Lauermann I, Lux-Steiner MC, Fischer C-H. Spray-ILGAR ZnS nanodots/In2S3 as defect passivation/point contact bilayer buffer for Cu(In,Ga)(S,Se)2 solar cells. *Solar Energy Materials and Solar Cells* 2013; **117**: 293–299. DOI: 10.1016/j.solmat.2013.06.007.

94 Koida T, Nishinaga J, Higuchi H, Kurokawa A, Iioka M, Kamikawa-Shimizu Y, Yamada A, Shibata H, Niki S. Comparison of ZnO:B and ZnO:Al layers for Cu(In,Ga)Se2 submodules. *Thin Solid Films*. DOI: 10.1016/j.tsf.2016.03.004.

95 Hála M, Fujii S, Redinger A, Inoue Y, Rey G, Thevenin M, Deprédurand V, Weiss TP, Bertram T, Siebentritt S. Highly conductive ZnO films with high near infrared transparency. *Progress in Photovoltaics: Research and Applications* 2015; **23**(11): 1630–1641. DOI: 10.1002/pip.2601.

96 Koida T, Fujiwara H, Kondo M. Hydrogen-doped In2O3 as High-mobility Transparent Conductive Oxide. *Japanese Journal of Applied Physics* 2007; **46**(No. 28): L685–L687. DOI: 10.1143/JJAP.46.L685.

97 Jäger T, Romanyuk YE, Nishiwaki S, Bissig B, Pianezzi F, Fuchs P, Gretener C, Döbeli M, Tiwari AN. Hydrogenated indium oxide window layers for high-efficiency Cu(In,Ga)Se2 solar cells. *Journal of Applied Physics* 2015; **117**(20): 205301. DOI: 10.1063/1.4921445.

98 Menner R, Cemernjak M, Paetel S, Wischmann W. Application of IndiumZinc Oxide Window Layers in Cu(In,Ga)Se2 Solar Cells. In Lille (France), 2016.

99 Feist R, Rozeveld S, Mushrush M, Haley R, Lemon B, Gerbi J, Nichols B, Nilsson R, Richardson T, Sprague S, Tesch R, Torka S, Wood C, Wu S, Yeung S, Bernius MT. Examination of lifetime-limiting failure mechanisms in CIGSS-based PV minimodules under environmental stress. In *33rd IEEE Photovoltaic Specialists Conference, 2008. PVSC '08*, 2008; 1–5. DOI: 10.1109/PVSC.2008.4922579.

100 Kempe MD, Terwilliger KM, Tarrant D. Stress induced degradation modes in CIGS mini-modules. In *33rd IEEE Photovoltaic Specialists Conference, 2008. PVSC '08*, 2008; 1–6. DOI: 10.1109/PVSC.2008.4922497.

101 Igalson M, Wimbor M, Wennerberg J. The change of the electronic properties of CIGS devices induced by the “damp heat” treatment. *Thin Solid Films* 2002; **403–404**: 320–324. DOI: 10.1016/S0040-6090(01)01510-3.

102 Kijima S, Nakada T. High-Temperature Degradation Mechanism of Cu(In,Ga)Se $_2$ -Based Thin Film Solar Cells. *Applied Physics Express* 2008; **1**: 75002. DOI: 10.1143/APEX.1.075002.

103 Lee D-W, Cho W-J, Song J-K, Kwon O-Y, Lee W-H, Park C-H, Park K-E, Lee H, Kim Y-N. Failure analysis of Cu(In,Ga)Se2 photovoltaic modules: degradation mechanism of Cu(In,Ga)Se2 solar cells under harsh environmental conditions. *Progress in Photovoltaics: Research and Applications* 2015; **23**(7): 829–837. DOI: 10.1002/pip.2497.

104 Theelen M, Boumans T, Stegeman F, Colberts F, Illiberi A, van Berkum J, Barreau N, Vroon Z, Zeman M. Physical and chemical degradation behavior of sputtered aluminum doped zinc oxide layers for Cu(In,Ga)Se2 solar cells. *Thin Solid Films* 2014; **550**: 530–540. DOI: 10.1016/j.tsf.2013.10.149.

105 Greiner D, Gledhill SE, Köble C, Krammer J, Klenk R. Damp heat stability of Al-doped zinc oxide films on smooth and rough substrates. *Thin Solid Films* 2011; **520**(4): 1285–1290. DOI: 10.1016/j.tsf.2011.04.190.

106 Hüpkes J, Owen JI, Wimmer M, Ruske F, Greiner D, Klenk R, Zastrow U, Hotovy J. Damp heat stable doped zinc oxide films. *Thin Solid Films* 2014; **555**: 48–52. DOI: 10.1016/j.tsf.2013.08.011.

107 Carcia PF, McLean RS, Hegedus S. Encapsulation of Cu(InGa)Se2 solar cell with Al2O3 thin-film moisture barrier grown by atomic layer deposition. *Solar Energy Materials and Solar Cells* 2010; **94**(12): 2375–2378. DOI: 10.1016/j.solmat.2010.08.021.

108 Sundaramoorthy R, Pern FJ, DeHart C, Gennett T, Meng FY, Contreras M, Gessert T. Stability of TCO window layers for thin-film CIGS solar cells upon damp heat exposures: part II. In vol 7412, 2009; 74120J–74120J–12. DOI: 10.1117/12.826604.

109 Coyle DJ, Blaydes HA, Northey RS, Pickett JE, Nagarkar KR, Zhao R-A, Gardner JO. Life prediction for CIGS solar modules part 2: degradation kinetics, accelerated testing, and encapsulant effects. *Progress in Photovoltaics: Research and Applications* 2013; **21**(2): 173–186. DOI: 10.1002/pip.1171.

110 Pern FJ, Noufi R, Li X, DeHart C, To B. Damp-heat induced degradation of transparent conducting oxides for thin-film solar cells. In *33rd IEEE Photovoltaic Specialists Conference, 2008. PVSC ’08*, 2008; 1–6. DOI: 10.1109/PVSC.2008.4922491.

111 Guillén C, Herrero J. Stability of sputtered ITO thin films to the damp-heat test. *Surface and Coatings Technology* 2006; **201**(1–2): 309–312. DOI: 10.1016/j.surfcoat.2005.11.114.

112 Romanyuk YE, Hagendorfer H, Stücheli P, Fuchs P, Uhl AR, Sutter-Fella CM, Werner M, Haass S, Stückelberger J, Broussillou C, Grand P-P, Bermudez V, Ti-

wari AN. All Solution-Processed Chalcogenide Solar Cells – from Single Functional Layers Towards a 13.8% Efficient CIGS Device. *Advanced Functional Materials* 2015; **25**(1): 12–27. DOI: 10.1002/adfm.201402288.

113 Tsin F, Venerosy A, Vidal J, Collin S, Clatot J, Lombez L, Paire M, Borensztajn S, Broussillou C, Grand PP, Jaime S, Lincot D, Rousset J. Electrodeposition of ZnO window layer for an all-atmospheric fabrication process of chalcogenide solar cell. *Scientific Reports* 2015; **5**: 8961. DOI: 10.1038/srep08961.

114 Crossay A, Buecheler S, Kranz L, Perrenoud J, Fella CM, Romanyuk YE, Tiwari AN. Spray-deposited Al-doped ZnO transparent contacts for CdTe solar cells. *Solar Energy Materials and Solar Cells* 2012; **101**: 283–288. DOI: 10.1016/j.solmat.2012.02.008.

115 Reinhard P, Buecheler S, Tiwari AN. Technological status of Cu(In,Ga)(Se,S)2-based photovoltaics. *Solar Energy Materials and Solar Cells* 2013; **119**: 287–290. DOI: 10.1016/j.solmat.2013.08.030.

116 16 percent: Manz achieves new world record for efficiency of CIGS thin-film solar modules | Manz AG.Accesed May 12, 2016http://www.manz.com/.

117 Green MA, Emery K, Hishikawa Y, Warta W, Dunlop ED. Solar cell efficiency tables (version 47). *Progress in Photovoltaics: Research and Applications* 2016; **24**(1): 3–11. DOI: 10.1002/pip.2728.

118 hanergy analysts report.hanergythinfilmpoweAccesed May 12, 2016http://www.hanergythinfilmpower.com/admin/media/anaytsts-report/20131121-quam-research-hanergy-solar-group--0566-hk-.pdf.

119 Siva Power Approaches 19% Efficiency in Record Time; Adds to Solar Company's Powerful Technical Advisory Board.Accesed May 12, 2016http://www.prnewswire.com/news-releases/siva-power-approaches-19-efficiency-in-record-time-adds-to-solar-companys-powerful-technical-advisory-board-243722021.html.

120 Wiedeman S, Albright S, Britt JS, Schoop U, Schuler S, Stoss W, Verebelyi D. Manufacturing ramp-up of flexible CIGS PV. In *2010 35th IEEE Photovoltaic Specialists Conference (PVSC)*, 2010; 003485–003490. DOI: 10.1109/PVSC.2010.5614725.

121 Ascent Solar - Ascent Solar Achieves 14 Percent Cell Efficiency Milestone in Commercial Production - October 21, 2009.October 21, 2009Accesed May 12, 2016http://investors.ascentsolar.com/releasedetail.cfm?ReleaseID=437180.

122 Nakamura M, Chiba Y, Kijima S, Horiguchi K, Yanagisawa Y, Sawai Y, Ishikawa K, Hakuma H. Achievement of 17.5% efficiency with 30 #x00D7; 30cm2-sized Cu(In,Ga)(Se,S)2 submodules. In *2012 38th IEEE Photovoltaic Specialists Conference (PVSC)*, 2012; 001807–001810. DOI: 10.1109/PVSC.2012.6317944.

123 MiaSolé - Home.MiaSoléAccesed May 12, 2016http://miasole.com/.

124 Technology - Midsummer.Accesed May 12, 2016http://midsummer.se/technology.

125 WonCIGS Current Status.Accesed May 12, 2016http://www.woncigs.com/bbs/content.php?co_id=Current.

126 NuvoSun™ FlexsoLyt™ | Dow.DOW solar NuvoSunAccesed May 12, 2016http://www.dowsolar.com/en/nuvosun/nuvosun-lightweight-flexible.

127 HULKet Energy takes CIGS module power to record 324 Watts.HULKet Energy CorporationJuly 7, 2015Accesed May 14, 2016http://www.hulket.com/?p=4277.

128 Stion Demonstrates 23.2% Efficiency Thin Film With Simply Better Tandem Technology.StionAccesed May 2, 2016http://www.stion.com/stion-demonstrates-23-2-efficiency-thin-film-with-simply-better-tandem-technology/.

129 Broussillou C, Viscogliosi C, Rogee A, Angle S, Grand PP, Bodnar S, Debauche C, Allary JL, Bertrand B, Guillou C, Parissi L, Coletti S. Statistical Process Control for Cu(In,Ga)(S,Se)2 electrodeposition-based manufacturing process of 60x120cm2 modules up to 14,0% efficiency. In *Photovoltaic Specialist Conference (PVSC), 2015 IEEE 42nd*, 2015; 1–5. DOI: 10.1109/PVSC.2015.7356224.

130 Aksu S, Pethe S, Kleiman-Shwarsctein A, Kundu S, Pinarbasi M. Recent advances in electroplating based CIGS solar cell fabrication. In *2012 38th IEEE Photovoltaic Specialists Conference (PVSC)*, 2012; 003092–003097. DOI: 10.1109/PVSC.2012.6318235.

131 Powalla M, Witte W, Jackson P, Paetel S, Lotter E, Wuerz R, Kessler F, Tschamber C, Hempel W, Hariskos D, Menner R, Bauer A, Spiering S, Ahlswede E, Friedlmeier TM, Blázquez-Sánchez D, Klugius I, Wischmann W. CIGS Cells and Modules With High Efficiency on Glass and Flexible Substrates. *IEEE Journal of Photovoltaics* 2014; **4**(1): 440–446. DOI: 10.1109/JPHOTOV.2013.2280468.

132 Hariskos D, Fuchs B, Menner R, Naghavi N, Hubert C, Lincot D, Powalla M. The Zn(S,O,OH)/ZnMgO buffer in thin-film Cu(In,Ga)(Se,S)2-based solar cells part II: Magnetron sputtering of the ZnMgO buffer layer for in-line co-evaporated Cu(In,Ga)Se2 solar cells. *Progress in Photovoltaics: Research and Applications* 2009; **17**(7): 479–488. DOI: 10.1002/pip.897.

133 Ward JS, Egaas B, Noufi R, Contreras M, Ramanathan K, Osterwald C, Emery K. Cu(In,Ga)Se2 solar cells measured under low flux optical concentration. In *2014 IEEE 40th Photovoltaic Specialist Conference (PVSC)*, 2014; 2934–2937. DOI: 10.1109/PVSC.2014.6925546.

134 CIGS Solar Cell with World's Highest Level Energy Conversion Efficiency.Toshiba R&D CenterAccesed May 11, 2016https://www.toshiba.co.jp/rdc/rd/fields/14_e06_e.htm.

135 Nishiwaki S, Burn A, Buecheler S, Muralt M, Pilz S, Romano V, Witte R, Krainer L, Spühler GJ, Tiwari AN. A monolithically integrated high-efficiency Cu(In,Ga)Se2 mini-module structured solely by laser. *Progress in Photovoltaics: Research and Applications* 2015: n/a-n/a. DOI: 10.1002/pip.2583.

136 Kamikawa Y, Nishinaga J, Ishizuka S, Shibata H, Niki S. Effects of Mo surface oxidation on Cu(In,Ga)Se $_2$ solar cells fabricated by three-stage process with KF postdeposition treatment. *Japanese Journal of Applied Physics* 2016; **55**(2): 22304. DOI: 10.7567/JJAP.55.022304.

137 Moriwaki K, Nomoto M, Yuuya S, Murakami N, Ohgoh T, Yamane K, Ishizuka S, Niki S. Monolithically integrated flexible Cu(In,Ga)Se2 solar cells and submodules using newly developed structure metal foil substrate with a dielectric layer. *Solar Energy Materials and Solar Cells* 2013; **112**: 106–111. DOI: 10.1016/j.solmat.2013.01.016.

138 Thompson CP, Chen L, Shafarman WN, Lee J, Fields S, Birkmire RW. Bandgap gradients in (Ag,Cu)(In,Ga)Se2 thin film solar cells deposited by three-stage co-evaporation. In *Photovoltaic Specialist Conference (PVSC), 2015 IEEE 42nd*, 2015; 1–6. DOI: 10.1109/PVSC.2015.7355692.

139 Nakamura M, Kouji Y, Chiba Y, Hakuma H, Kobayashi T, Nakada T. Achievement of 19.7% efficiency with a small-sized Cu(InGa)(SeS)2 solar cells prepared by sulfurization after selenizaion process with Zn-based buffer. In *2013 IEEE 39th Photovoltaic Specialists Conference (PVSC)*, 2013; 0849–0852. DOI: 10.1109/PVSC.2013.6744278.

140 Kobayashi T, Yamaguchi H, Nakada T. Effects of combined heat and light soaking on device performance of Cu(In,Ga)Se2 solar cells with ZnS(O,OH) buffer layer. *Progress in Photovoltaics: Research and Applications* 2014; **22**(1): 115–121. DOI: 10.1002/pip.2339.

141 Haarstrich J, Metzner H, Oertel M, Ronning C, Rissom T, Kaufmann CA, Unold T, Schock HW, Windeln J, Mannstadt W, Rudigier-Voigt E. Increased homogeneity and open-circuit voltage of Cu(In,Ga)Se2 solar cells due to higher deposition temperature. *Solar Energy Materials and Solar Cells* 2011; **95**(3): 1028–1030. DOI: 10.1016/j.solmat.2010.10.021.

142 Merdes S, Ziem F, Lavrenko T, Walter T, Lauermann I, Klingsporn M, Schmidt S, Hergert F, Schlatmann R. Above 16% efficient sequentially grown Cu(In,Ga)(Se,S)2-based solar cells with atomic layer deposited Zn(O,S) buffers. *Progress in Photovoltaics: Research and Applications* 2015: n/a-n/a. DOI: 10.1002/pip.2579.

143 Wallin E, Malm U, Jarmar T, Edoff OL Marika, Stolt L. World-record Cu(In,Ga)Se2-based thin-film sub-module with 17.4% efficiency. *Progress in Photovoltaics: Research and Applications* 2012; **20**(7): 851–854. DOI: 10.1002/pip.2246.

144 Bhattacharya RN. CIGS-based solar cells prepared from electrodeposited stacked Cu/In/Ga layers. *Solar Energy Materials and Solar Cells* 2013; **113**: 96–99. DOI: 10.1016/j.solmat.2013.01.028.

145 Todorov TK, Gunawan O, Gokmen T, Mitzi DB. Solution-processed Cu(In,Ga)(S,Se)2 absorber yielding a 15.2% efficient solar cell. *Progress in Photovoltaics: Research and Applications* 2013; **21**(1): 82–87. DOI: 10.1002/pip.1253.

146 Vos AD. Detailed balance limit of the efficiency of tandem solar cells. *Journal of Physics D: Applied Physics* 1980; **13**(5): 839. DOI: 10.1088/0022-3727/13/5/018.

147 Bremner SP, Levy MY, Honsberg CB. Analysis of tandem solar cell efficiencies under AM1.5G spectrum using a rapid flux calculation method. *Progress in Photovoltaics: Research and Applications* 2008; **16**(3): 225–233. DOI: 10.1002/pip.799.

148 Wu X, Zhou J, Duda A, Keane JC, Gessert T a., Yan Y, Noufi R. High-Efficiency CdTe Polycrystalline Thin-Film Solar Cells with an Ultra-Thin CuxTe Transparent Back-Contact. In *Symposium F – Thin-Film Compound Semiconductor Photovoltaics*, vol 865, 2005; F114 (6 pages). DOI: 10.1557/PROC-865-F114.

149 Kranz L, Abate A, Feurer T, Fu F, Avancini E, Löckinger J, Reinhard P, Zakeeruddin SM, Grätzel M, Buecheler S, Tiwari AN. High-Efficiency Polycrystalline Thin Film Tandem Solar Cells. *The Journal of Physical Chemistry Letters* 2015; **6**(14): 2676–2681. DOI: 10.1021/acs.jpclett.5b01108.

150 Todorov T, Gershon T, Gunawan O, Lee YS, Sturdevant C, Chang L-Y, Guha S. Monolithic Perovskite-CIGS Tandem Solar Cells via In Situ Band Gap Engineering. *Advanced Energy Materials* 2015; **5**(23). DOI: 10.1002/aenm.201500799.

151 Moon SH, Park SJ, Kim SH, Lee MW, Han J, Kim JY, Kim H, Hwang YJ, Lee D-K, Min BK. Monolithic DSSC/CIGS tandem solar cell fabricated by a solution process. *Scientific Reports* 2015; **5**. DOI: 10.1038/srep08970.

152 Wenger S, Seyrling S, Tiwari AN, Grätzel M. Fabrication and performance of a monolithic dye-sensitized TiO2/Cu(In,Ga)Se2 thin film tandem solar cell. *Applied Physics Letters* 2009; **94**(17): 173508. DOI: 10.1063/1.3125432.

153 Bailie CD, Christoforo MG, Mailoa JP, Bowring AR, Unger EL, Nguyen WH, Burschka J, Pellet N, Lee JZ, Grätzel M, Noufi R, Buonassisi T, Salleo A, McGehee MD. Semi-transparent perovskite solar cells for tandems with silicon and CIGS. *Energy Environ. Sci.* 2015; **8**(3): 956–963. DOI: 10.1039/C4EE03322A.

154 Fu F, Feurer T, Jäger T, Avancini E, Bissig B, Yoon S, Buecheler S, Tiwari AN. Low-temperature-processed efficient semi-transparent planar perovskite solar cells for bifacial and tandem applications. *Nature Communications* 2015; **6**: 8932. DOI: 10.1038/ncomms9932.

155 New world record for solar cell efficiency at 46% — Fraunhofer ISE.Accesed May 23, 2016https://www.ise.fraunhofer.de/en/press-and-media/press-releases/press-releases-2014/new-world-record-for-solar-cell-efficiency-at-46-percent.

156 Paire M, Shams A, Lombez L, Péré-Laperne N, Collin S, Pelouard J-L, Guillemoles J-F, Lincot D. Resistive and thermal scale effects for Cu(In, Ga)Se2 polycrystalline thin film microcells under concentration. *Energy & Environmental Science* 2011; **4**(12): 4972. DOI: 10.1039/c1ee01661j.

157 Virtuani A, Lotter E, Powalla M. Performance of Cu(In,Ga)Se-2 solar cells under low irradiance. *Thin Solid Films* 2003; **431**: 443–447. DOI: 10.1016/S0040-6090(03)00184-6.

158 Powalla M, Hariskos D, Lotter E, Oertel M, Springer J, Stellbogen D, Dimmler B, Schaffler R. Large-area CIGS modules: processes and properties. *Thin Solid Films* 2003; **431**: 523–533. DOI: 10.1016/S0040-6090(03)00255-4.

159 Fecher FW, Romero AP, Brabec CJ, Buerhop-Lutz C. Influence of a shunt on the electrical behavior in thin film photovoltaic modules - A 2D finite element simulation study. *Solar Energy* 2014; **105**: 494–504. DOI: 10.1016/j.solener.2014.04.011.

160 Virtuani A, Lotter E, Powalla M, Rau U, Werner JH. Highly resistive Cu(In,Ga)Se-2 absorbers for improved low-irradiance performance of thin-film solar cells. *Thin Solid Films* 2004; **451**: 160–165. DOI: 10.1016/j.tsf.2003.10.094.

161 Virtuani A, Lotter E, Powalla M, Rau U, Werner JH, Acciarri M. Influence of Cu content on electronic transport and shunting behavior of Cu(In,Ga)Se-2 solar cells. *Journal of Applied Physics* 2006; **99**. DOI: Artn 014906 10.1063/1.2159548.

162 Wang X, Ehrhardt M, Lorenz P, Scheit C, Ragnow S, Ni XW, Zimmer K. The influence of the laser parameter on the electrical shunt resistance of scribed Cu(InGa)Se-2 solar cells by nested circular laser scribing technique. *Applied Surface Science* 2014; **302**: 194–197. DOI: 10.1016/j.apsusc.2013.10.155.

163 Wennerberg J, Kessler J, Stolt L. Cu(In,Ga)Se-2-based thin-film photovoltaic modules optimized for long-term performance. *Solar Energy Materials and Solar Cells* 2003; **75**: 47–55. DOI: Pii S0927-0248(02)00101-0 Doi 10.1016/S0927-0248(02)00101-0.

164 Brecl K, Topic M, Smole F. A detailed study of monolithic contacts and electrical losses in a large-area thin-film module. *Progress in Photovoltaics* 2005; **13**: 297–310. DOI: 10.1002/pip.589.

165 Wehrmann A, Schulte-Huxel H, Ehrhardt M, Ruthe D, Zimmer K, Braun A, Ragnow S. Change of electrical properties of CIGS thin-film solar cells after structuring with ultrashort laser pulses. *Laser-Based Micro- and Nanopackaging and Assembly V* 2011; **7921**. DOI: Artn 79210t 10.1117/12.874999.

166 Ralph E, Woike T. Solar cell array system trades - Present and future. In *37th Aerospace Sciences Meeting and Exhibit*, American Institute of Aeronautics and Astronautics, 1999.

167 Stevens NJ. Solar array experiments on the Sphinx satellite. In 13-15 Nov. 1973, United States, 1973.

168 Dhere NG, Ghongadi SR, Pandit MB, Jahagirdar AH, Scheiman D. CIGS2 thin-film solar cells on flexible foils for space power. *Progress in Photovoltaics: Research and Applications* 2002; **10**(6): 407–416. DOI: 10.1002/pip.447.

169 Tringe J, Merrill J, Reinhardt K. Developments in thin-film photovoltaics for space. In *Conference Record of the Twenty-Eighth IEEE Photovoltaic Specialists Conference, 2000*, 2000; 1242–1245. DOI: 10.1109/PVSC.2000.916114.

170 Space Technologies Studies 2014: Results.Swiss Space Office project reportFebruary 16, 2016Accesed May 24, 2016http://space.epfl.ch/files/content/sites/space/files/shared/space_center/Events/MdP%202014%20Full%20Abstract%20book.pdf.

171 First Solar adding factory integrated three module systems for trackers.PV-TechAccesed May 8, 2016http://www.pv-tech.org/news/first-solar-adding-factory-integrated-three-module-systems-for-trackers.

172 Nagy Z, Svetozarevic B, Jayathissa P, Begle M, Hofer J, Lydon G, Willmann A, Schlueter A. The Adaptive Solar Facade: From concept to prototypes. *Frontiers of Architectural Research*. DOI: 10.1016/j.foar.2016.03.002.

173 Rüggeberg M, Burgert I. Bio-Inspired Wooden Actuators for Large Scale Applications. *PLOS ONE* 2015; **10**(4): e0120718. DOI: 10.1371/journal.pone.0120718.

Figures (to be separated)

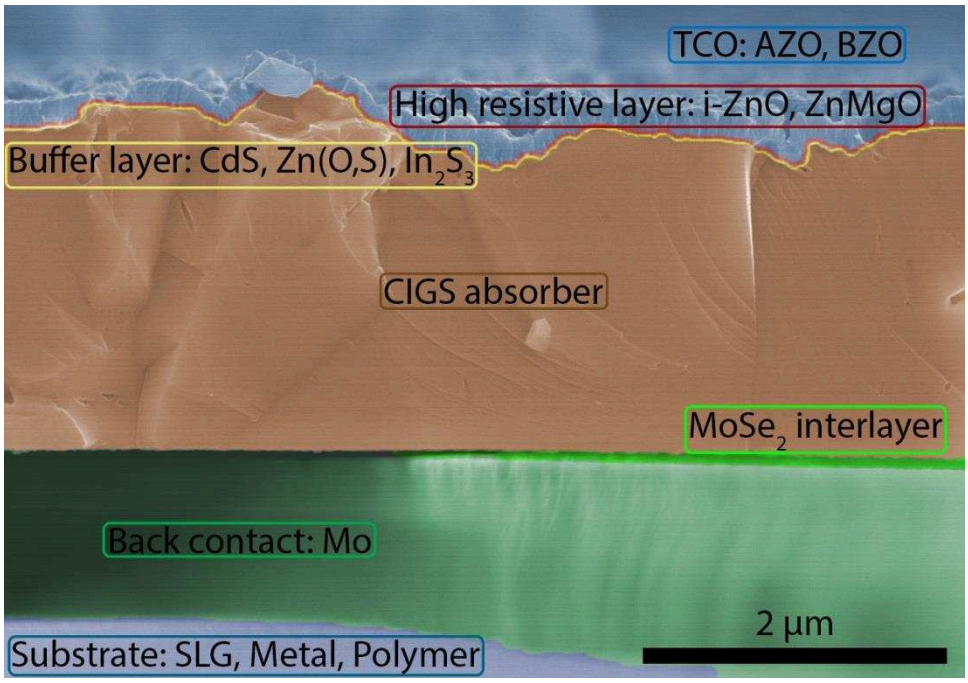

Figure 1: Basic structure of a typical CIGS solar cell, with examples of the most commonly used materials.

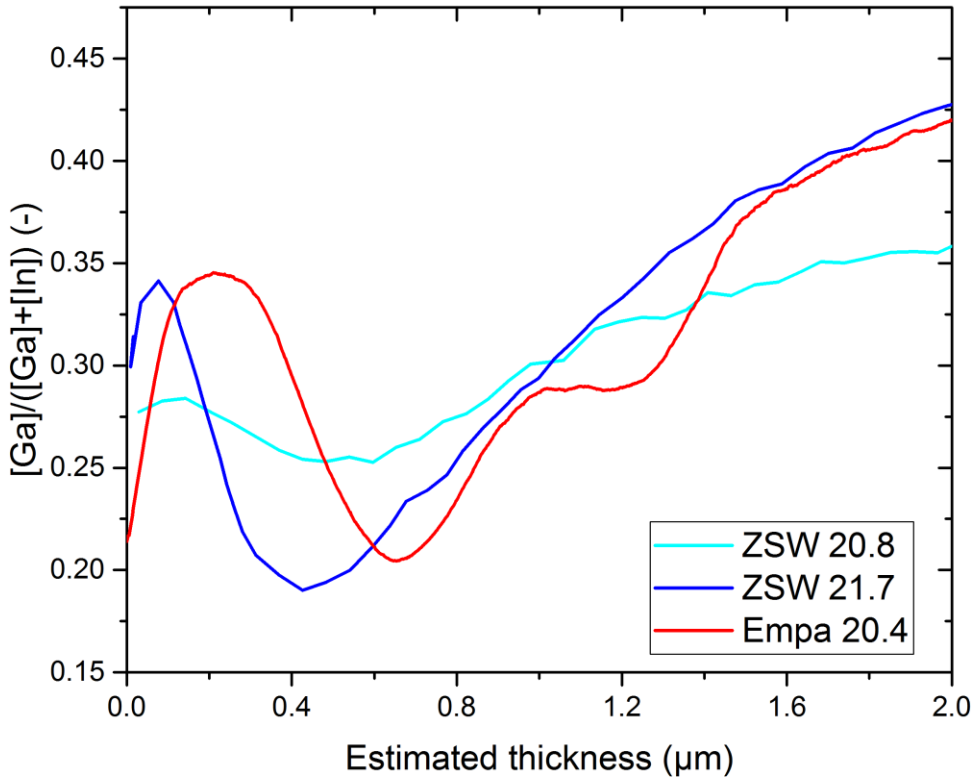

Figure 2: Comparison of published [Ga]/([Ga]+[In]) gradings in CIGS solar cells with efficiency > 20 % [10,12].

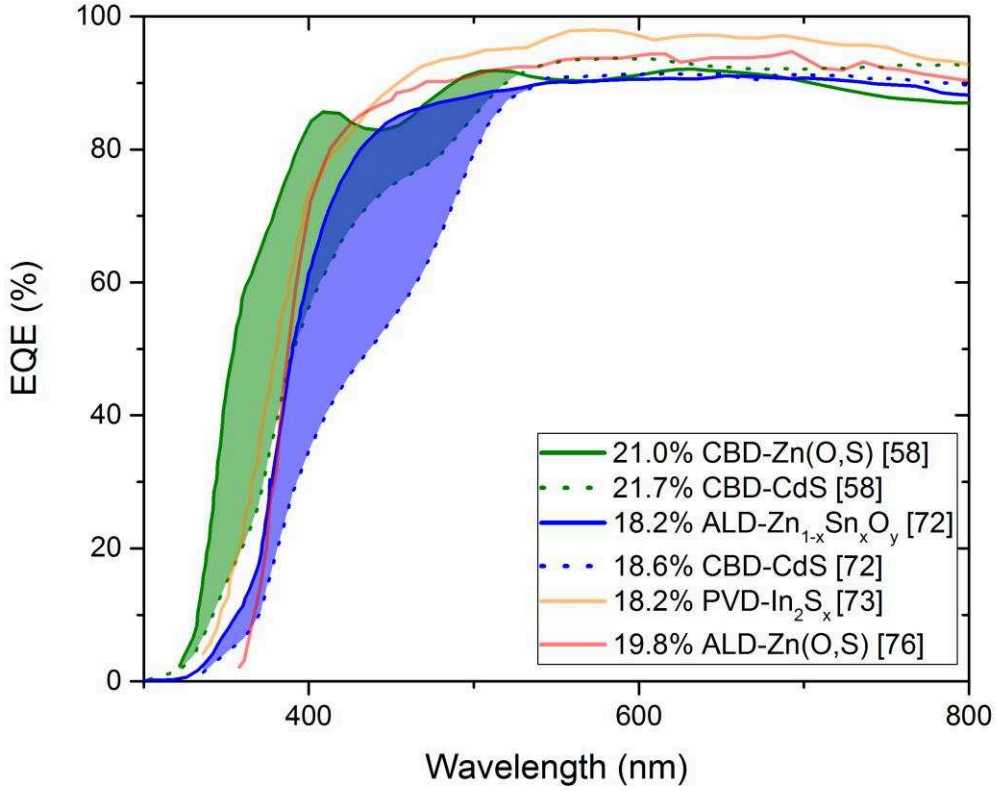

Figure 3: EQE for CIGS cells with different buffer materials. All cells with anti-reflection coatings. The shaded areas below the curves represent the current gain relative to the corresponding CdS reference when available. Data extracted from [58,72,73,76].

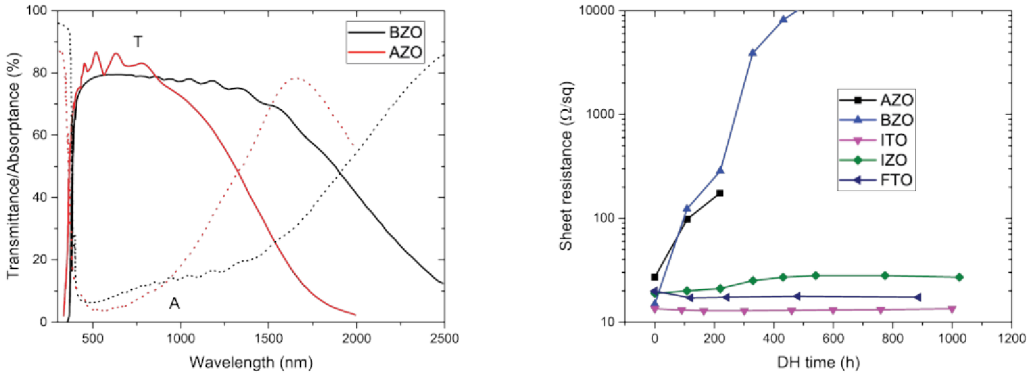

Figure 4: Left: Comparison of the optical properties of AZO and BZO with comparable sheet resistance. The high transmission in the NIR region for BZO stems from the reduced carrier density (AZO $n=4.4*10^{20}$ cm^{-3}, BZO $n=9.2*10^{19}$ cm^{-3}). (Adapted from [94]) Right: Damp heat stability (85°C, 85% r.h.) of different, non-encapsulated TCO materials (extracted from [108,110,111])

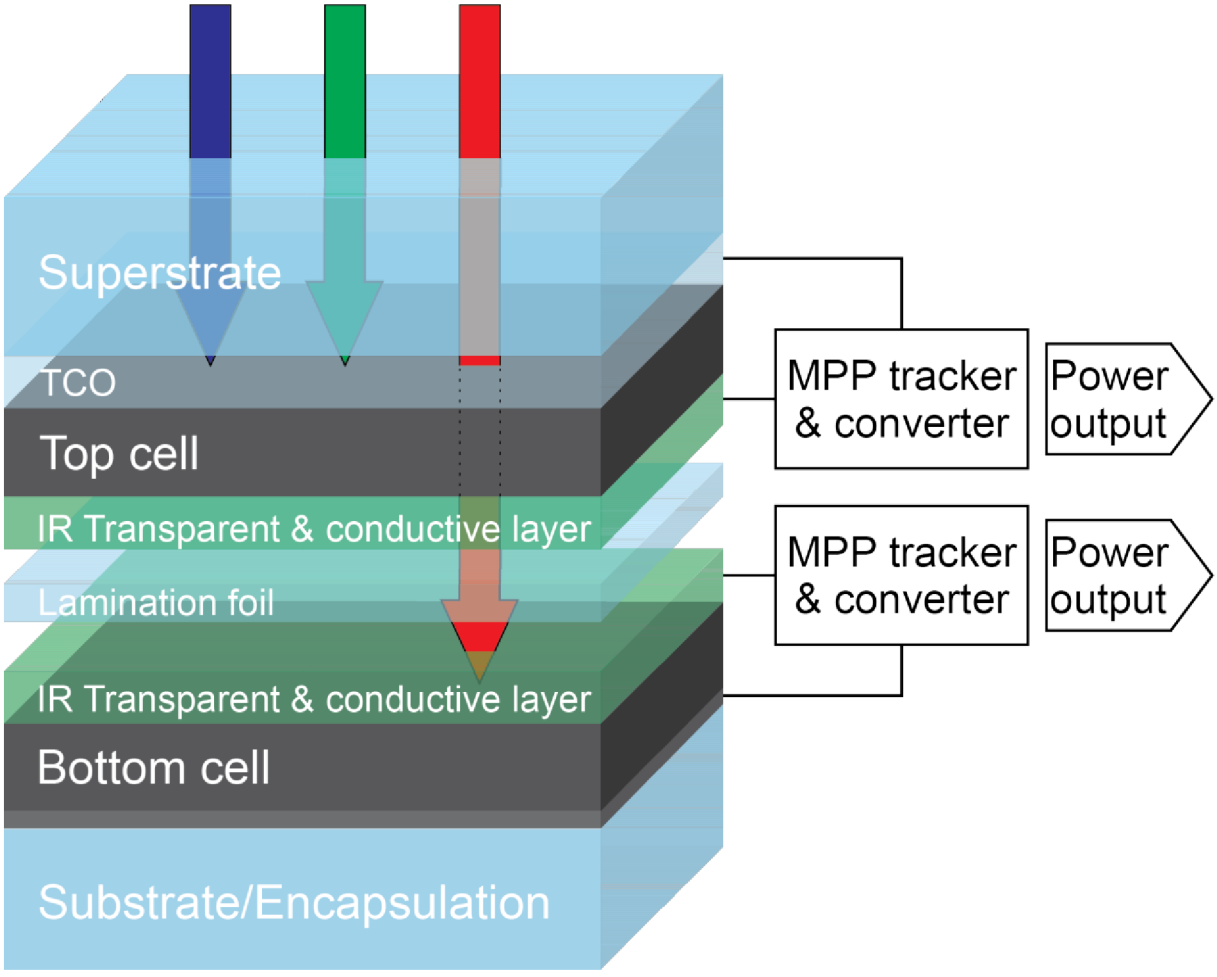

Figure 5: Schematic structure of a 4-terminal tandem structure. CIGS thin film solar cells are a suitable candidate for bottom cell while further research is required to find a suitable top cell.

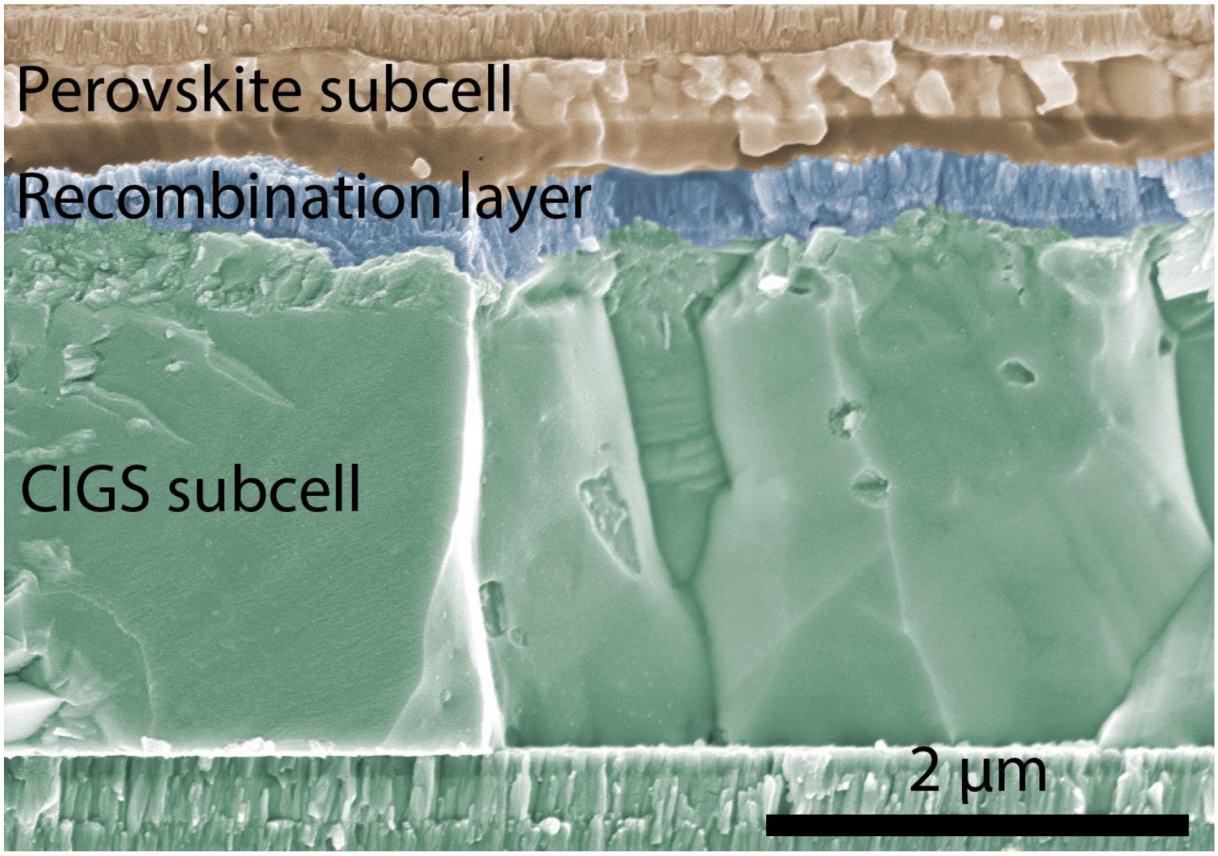

Figure 6: SEM cross-section of a monolithic Perovskite/CIGS tandem device with both cells and the recombination layer highlighted in color.

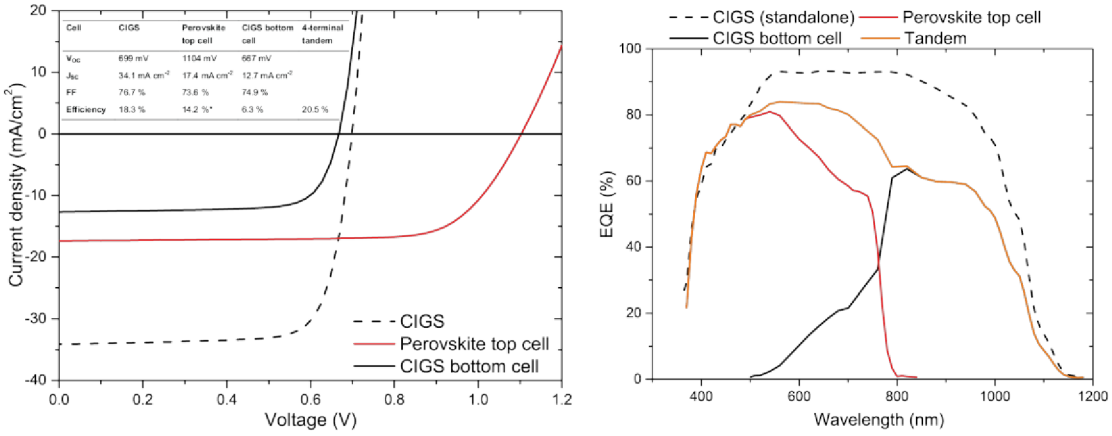

Figure 7: IV and EQE curves of the highest reported 4-terminal CIGS tandem. * The perovskite efficiency is measured by maximum power point tracking to exclude hysteresis effects [154].

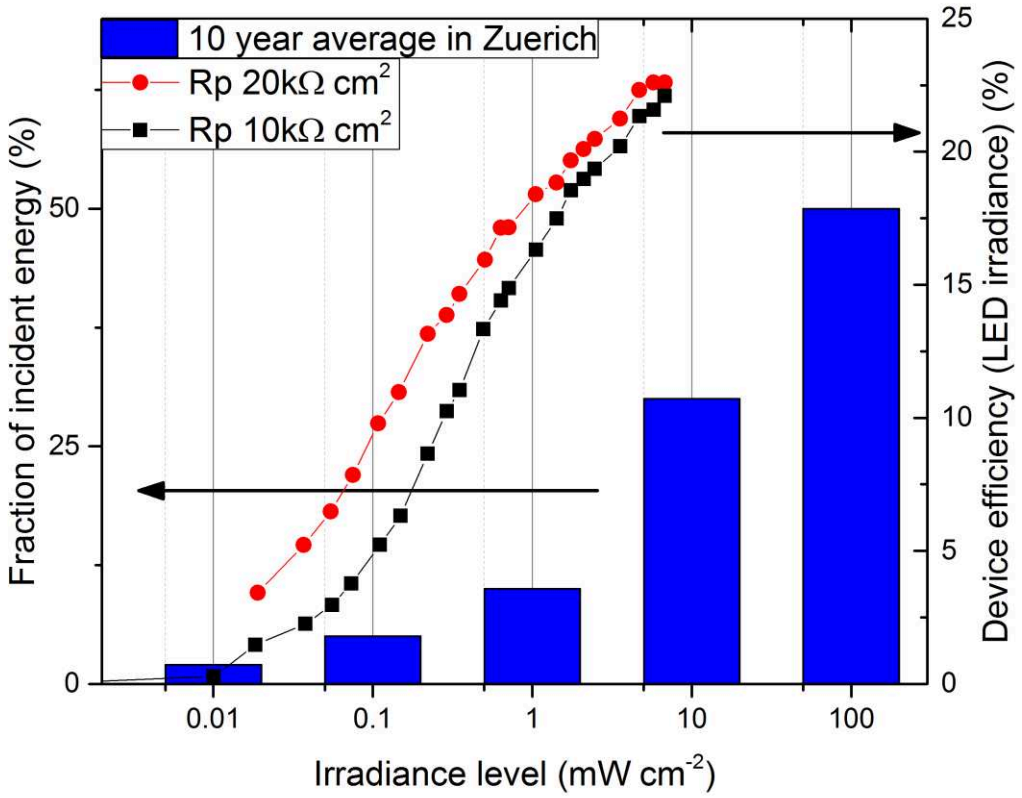

Figure 8: Distribution of incident energy at different irradiance levels on a 10 year average, data measured in Zurich (Switzerland). The curves show the efficiency of CIGS solar cells with different parallel resistances under LED irradiation for application under low light or indoor illumination. The cell area for these devices was 0.27 cm^2.

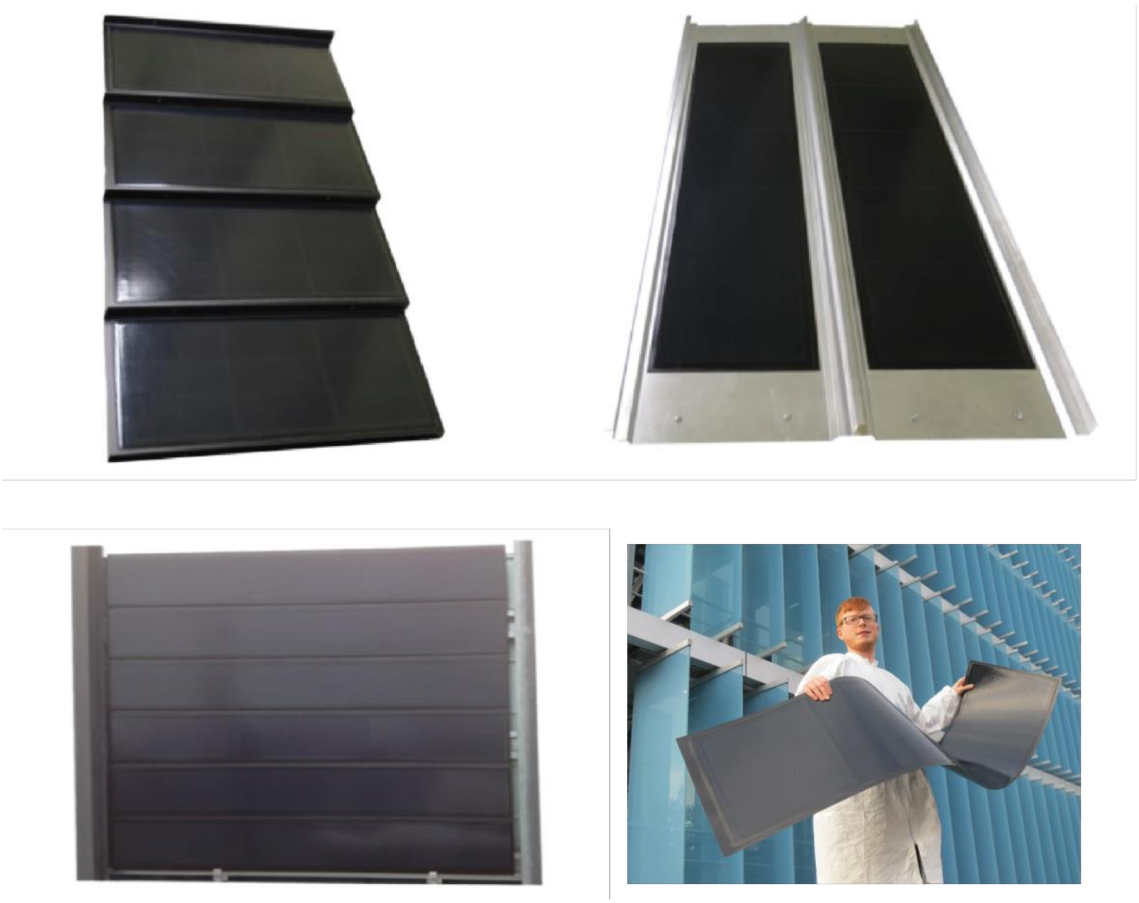

Figure 9: BIPV product concepts based on flexible, lightweight monolithic CIGS solar modules on polyimide, from top left to bottom left: Residential roof tile, architectural standing seam roof, metal façade cladding elements. Bottom right: fully rollable module for application on rooftop membrane. All images courtesy of Flisom AG.

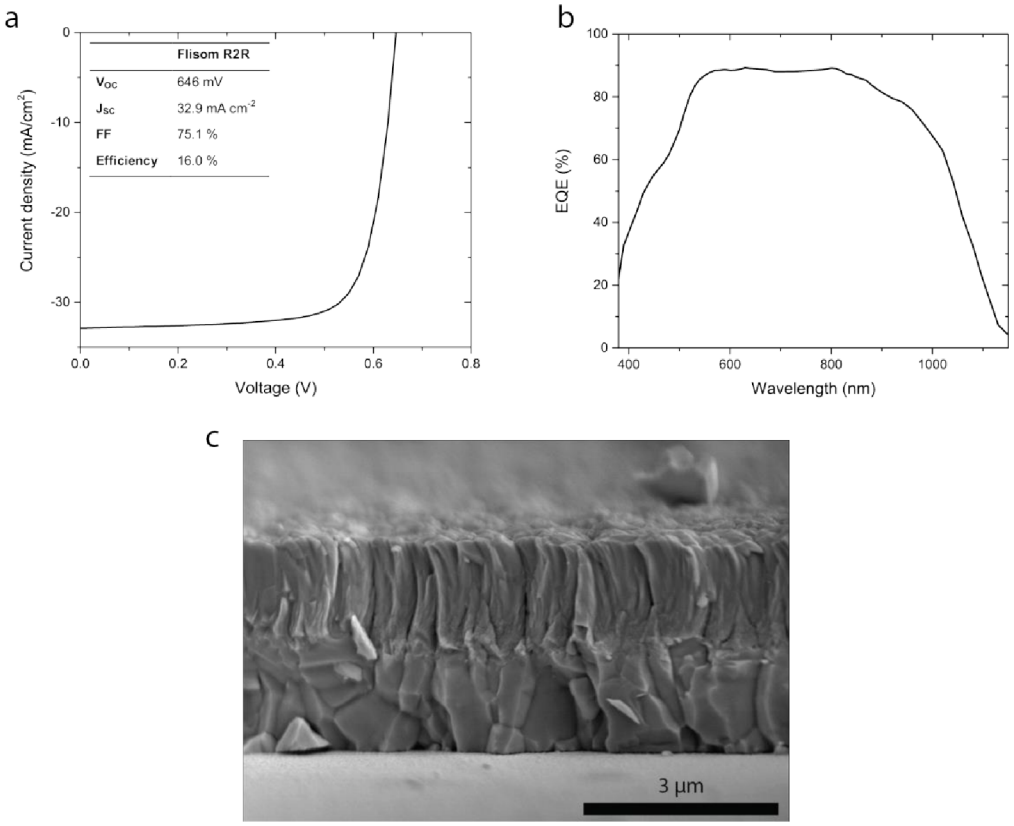

Figure 10: a) IV and b) EQE curves of a solar cell based on a CIGS absorber deposited in a roll-to-roll process. Inset shows the IV parameters. c) SEM cross section of a fully roll-to-roll processed solar cell.

Tables

Table 1: Published efficiencies for a selection of industrial producers. Updated from earlier work [115]. Data for companies not existing anymore is not included. Status: published results until July 2016

Deposition method		Company	Absorber material	Substrate[1]	Cells intercon.[2]	Reported η [%] (area[3] [cm^2])		Ref. (for η)	Notes
						Cell	Module (M)/ Submodule (S)		
Vacuum-based (direct growth)	Co-evaporation	Manz - Würth Solar	CIGSe	Glass	Monol.	22.6*	16.0 M	[1,116]	Collaboration with ZSW
	Co-evaporation	Solibro (Hanergy)	CIGSe	Glass	Monol.	21.0*	15.6 (~1m2) M, 18.7* (16ap) S	[117,118]	Record submod.: monol. & grid
	Co-evaporation	Siva Power	CIGSe	Glass	Monol.	18.8* (0.5)		[119]	
	Co-evaporation	Flisom	CIGSe	PI	Monol.		16.9 (10.2da) S	[25]	Submod. with Empa
	Co-evaporation	Global Solar Energy (Hanergy)	CIGSe	SS	String	17.7° (1.0 ta) 15.5* (0.4ap)	14.7° (7870ap) 13.2* (3883ap) S	[120]	R2R, Flexible and rigid modules
	Co-evaporation	Ascent Solar (TFG Radiant)	CIGSe	PI	Monol.	14*	11.7 M	[121]	-
Vacuum-based precursor	Sputtering, selenization & sulfurization	Solar Frontier - Showa Shell	CIGSSe	Glass	Monol.	22.8°, 22.3* (0.5da)	17.8 (819ap) S, 17.5* (837.3ap) S, 14.6* (1.228 m^{2}ta) M	[13,14,122]	Zn(O,S,OH) buffer layer, collab. with NEDO
	Sputtering & RTP[4] (SEL-RTP process)	Avancis (CNBM)	CIGSSe	Glass	Monol.		17.9* (622ap)	[75]	SiN diffusion barrier

	Sputtering & selenization	Miasolé (Hanergy)	CIGSe	SS	Shingle	17	16.6° (ap) M 15.5* (1.68m^{2}ap) M	[123]	R2R, all-sputtering process
	Sputtering & selenization	Midsummer	CIGSe	SS	String	17.0 (ap)		[124]	Production line for cells (156 x156 mm), Cd free
	Sputtering, selenization & sulphurisation	WonCIGS	CIGSSe	Glass	Monol.		16.0* (1.445m^{2}ta) M, 16.8 (ap) M	[125]	Zn(O,S) buffer, "turn-key producer"
	Sputtering & selenization	NuvoSun (Dow)	CIGSe	SS	String	14 (268)	12.3 (3.555m^{2}ta) M	[126]	Flexible
	Rapid diffusion annealing of precursor	HULKet	CIGSe?	Glass	Monol.		13.8* (2.348m^{2}ta)M	[127]	ZnOx buffer
	Sputtering, selenization & sulphurisation	Stion	CIGSSe	Glass	Monol.	23.2	20 (tandem)	[128]	tandem solar cells
Non-vacuum-based pre-cursor	Electrodeposition & RTP	Nexcis	CIGSSe	Glass		17.3 (0.5)*	14.0* (0.7m^{2}ap) M	[129]	Collab. with IRDEP
	Electrodeposition & selenization	Solopower	CIGSe	SS	Shingle	15.36 (5.4ap)	13.4* (3824.6ap) M	[130]	

[1] PI = polyimide. SS = stainless steel. () = no clear information on substrate material; [2] Monol.: monolithic; [3] ap = aperture area. t = total area. da = designated illumination area; [4] rapid thermal processing; * externally certified efficiency; ° presented at IW-CIGSTech 7

Table 2: State of the art efficiencies on cell and sub-module level in selected research laboratories. Status: published results until July 2016

Institute	**Country**	**Cell η [%]**	**Ref. cell η**	**Sub-module η [%] (area[1] [cm^2])**	**Cells in-tercon.**	**Ref. sub-mod. η**	**CIGS deposi-tion method**	**Sub-strate[3]**	**Notes**
Solar Frontier	Japan	22.8° , 22.3*	[14]	17.8 (819ap)	monol.	[13]	Sputtering, selenization & sulfurization (CIGSSe)	Glass	With NEDO and AIST
ZSW	Germany	22.6*	[1]	16.8* (61ap)	monol.	[131]	Co-evaporation (CIGSe)	Glass	-
		21.0*	[58]	15.2 (63ap)	monol.	[132]	Co-evaporation (CIGSe)	Glass	Zn(O,S) buffer layer
NREL	USA	20.8	[133]	-	-	-	Co-evaporation (CIGSe)	Glass	-
		18.6	[22]	-	-	-	Evaporation & selenization	Glass	Zn(O,S) buffer layer
Toshiba	Japan	20.7	[134]	-	-	-	Co-evaporation (CIGSe)	Glass	-
Empa	CH	20.4*	[10]	16.6* (13ap)	monol. [2]	[135]	Co-evaporation (CIGSe)	PI	Flexible polyi-mide, module with Flisom
AIST	Japan	19.9	[136]	15.9* (69.6 da)	monol.	[137]	Co-evaporation (CIGSe)	Glass/SS	Monol. Interconn. on metal foil
IEC Delaware	USA	19.9	[138]	-	-		Co-evaporation (AgCIGSe)	PI	Wide band gap (Ag,Cu)(In,Ga)Se$_2$
AGU	Japan	19.7*	[139]	17.8 (819ap)	monol.	[122]	Sputtering, selenization & sulfurization (CIGSSe)	Glass	Zn(O,S) buffer layer, with Solar Frontier
		18.4	[140]	-			Co-evaporation (CIGSe)	Glass	Zn(O,S) buffer layer

		19.4*	[141]	-			Co-evaporation (CIGSe)	Glass	High growth temperature (>600°C)
HZB	Germany	16.1*	[142]	13.0 (30x30)	monol.	[142]	Sputtering, selenization & sulfurization (CIGSSe)		Zn(O,S) buffer layer, with Bosch
Uppsala	Sweden	18.6	[72]	17.4* (16ap)	monol.	[143]	Co-evaporation (CIGSe)	Glass	In-line, module with Solibro
Korea University	Korea	-	-	17.9 (900)	monol.	[74]	Sputtering, selenization & sulfurization (CIGSSe)	Glass	Zn(O,S) Buffer, with Samsung SDU
IRDEP	France	17.3*	[129]	14.0* (6610ap)	monol.	[129]	Electrodeposition and selenisation (CIGSSe)	Glass	Solution-based precursor, with Nexcis
NREL	USA	11.7*	[144]	-	-		Electrodeposition & selenization (CIGSe)	Glass	Solution-based precursor
IBM	USA	15.2*	[145]	-	-		Hydrazine-based (CIGSSe)	Glass	Pure solution

[1] ap = aperture area. t = total area. da = designated illumination area; [2] monolithic;[3] PI = polyimide. SS = stainless steel; *externally certified efficiency; ° presented at IW-CIGSTech 7

Table 3 Summary of best performing small-area CIGS cells with different buffer layers and respective deposition methods.

Buffer layer	Dep. method	Absorber	Window layer	Eff. (%)	V_{OC} (V)	J_{SC} (mA cm^{-2})	FF (%)	Area (cm^2)	ref
CdS	CBD	CIGSe	i-ZnO/ZnO:Al	21.7 *	0.746	36.6	79.3	0.5	[12]
Zn(O,S)	CBD	CIGSe	$Zn_{0.75}Mg_{0.25}O$/ ZnO:Al	21.0*	0.717	37.2	78.6	0.5	[58]
Zn(O,S)	CBD	CIGSSe	ZnO:B	17.9 *	0.66 (/cell calc.)	38.1	71.1	900	[74]
Zn(O,S)	ALD	CIGSe	ZnO:B	19.8 *	0.715	36.5	75.8	0.522	[76]
Zn(O,S)	Sputtering	CIGSe	ZnO:Al	18.3 *	0.654	38.4	72.8	0.49	[70]
$Zn_{1-x}Mg_xO$	ALD	CIGS	i-ZnO/ In_2O_3:Sn	15.5 *	0.92	23.4	72.2	0.433	[54]
$Zn_{1-x}Mg_xO$	ALD	CIGSe	i-ZnO/ZnO:Al	18.1	0.668	35.7	75.7	0.5	[71]
In_xS_y	Thermal evaporation	CIGSe	i-ZnO/ZnO:Al	18.2	0.673	36.3	74.5	0.5	[73]
$Zn_{1-x}Sn_xO_y$	ALD	CIGSe	i-ZnO/ZnO:Al	18.2 *	0.689	35.1	75.3	0.49	[72]

* externally certified efficiency

Table 4: Estimated specific power of a flexible CIGS thin film module assuming different substrate, support and front-encapsulation materials.

Substrate + mechanical support		CIGS PV cell	Front encapsulation (50 µm)	sum	Power / Weight ratio @ 15 % Eff in space (1360W/m2)
	g / m^2	g / m^2	g / m^2	g / m^2	kW/kg
Pi 25 µm	35	15	none	50	4.1
PI 25 µm + CFRP 200 µm	35 + 320	15	110 (FEP)	470	0.43
Titanium 100 µm	450			565	0.36
Steel 100 µm	780			895	0.23
Steel 100 µm	780	15	125 (glass)	920	0.22
Steel 127 µm			none	1000	0.20 [168]